Development of a Hybrid Photo-bioreactor coupled with Nano- and Micro-Interfaces for Air Pollution Remediation

Andrea Rocha

Department of Atmospheric and Oceanic Sciences

McGill University, Montreal

August 2016

A thesis submitted to McGill University in partial fulfillment of the requirements of the degree of Master of Science

Abstract

Carbon dioxide is one of the main greenhouse gases, known to contribute to global warming. A major source of anthropogenic CO_2 is from the combustion of fossil fuels, hence the application of mitigation techniques on combustion processes to capture CO_2 are of great importance to reduce emissions being released to the atmosphere. Photo-bioreactors with microalgae have demonstrated a potential for CO_2 fixation. However, they can present several drawbacks including the formation of side products or airborne particles (aerosols). These can have a negative impact on the climate and human health, if released to the atmosphere. I present the development of an algal photo-bioreactor system coupled with natural nano- and micro-particle interfaces containing iron oxides and alumina, which has the potential to remediate gaseous by-products at the source while reducing CO_2 emissions. The system uses recyclable nanoparticles, and can be operable using solar energy. Furthermore, to manage the algal waste produced from the photo-bioreactor, preliminary absorption tests were performed which demonstrated the potential of algae to serve as a biosorbent for remediation of gaseous mercury, a pollutant also present in flue gas emissions. A feasibility cost analysis was also performed to analyze the cost-effectiveness of the set-up and its up-scaling potential to couple it to existing industrial setups.

Résumé

Le dioxyde de carbone est l’un des principaux gaz à effet de serre, et contribue au réchauffement climatique. L’une des sources anthropiques majeures de CO_2 est la combustion des carburants fossiles, d’où l’importance de l’application de techniques de mitigation sur les processus de combustion, afin de capturer le CO_2 et réduire les émissions dans l’atmosphère. Les photo-bioréacteurs avec des micro-algues ont démontré un potentiel pour la fixation de CO_2. Toutefois, ils présentent plusieurs désavantages donc la formation de sous-produits ou des particules aériennes (aérosols). Ceux-ci peuvent avoir un impact négatif sur le climat et la santé humaine s’ils sont relâchés dans l’atmosphère. Je présente le développement d’un système de photo-bioréacteur avec des algues couplé avec des interfaces de nano- et microparticules naturels contenant des oxydes de fer et d’aluminium, ce qui a le potentiel de remédier aux sous-produits gazeux à la source tout en réduisant les émissions de CO_2. Le système utilise des nanoparticules recyclables et peut fonctionner à l’énergie solaire. De plus, afin de gérer les déchets algaux du photo-bioréacteur, des tests d’absorption préliminaires ont été effectués qui démontrent le potentiel des algues dans le rôle de biosorbent pour remédier au mercure gazeux, un polluant aussi présent dans les émissions de gaz de combustion. Une étude de faisabilité a aussi été effectuée afin d’étudier la viabilité économique de l’installation ainsi que son potentiel de mise à échelle pour l’associer à des installations industrielles.

Acknowledgments

I am beyond grateful to my mentor and supervisor Prof. Parisa Ariya, for her invaluable help and guidance throughout my journey at McGill University. Thank you very much to Dr. Hu and Uday for their supervision and help with laboratory procedures. Thank you also to group members: Jim, Rodrigo, Yevgen, Roya, and Greg. And to past members including Nermin, Ali, Connie, and Usman; among many others who have contributed to my amazing experience throughout my degree.

I am very grateful to Rick and the Electronics shop for all the help and patience with the solar panels, lighting and electronics work. I would also like to thank Mr. Georges Kopp for manufacturing my custom-made glass probes. I am grateful to Kelly and the Microscopy facility for the imaging of samples. Thank you to Jean Philippe from the Mechanics shop, for helping with any set-up repairs when necessary. Also, thank you to Terri Kafyeke for helping me with the translation of my abstract.

Finally, thank you to my dog and my sister, who were always there for me; and to my parents for their unconditional love and support.

Contribution of Authors

The format of my thesis is manuscript-based. The Introduction, Experimental Setup and Methodology of my work are presented, followed by the paper which is included in the Results and Discussion section. Dr. Hu contributed to the manuscript with the section on the characterization of nanoparticles. The manuscript that I have written is a build-up of a project that started with a previous Master's student, Christian Wilde. His focus was on the photo-bioreactor, to demonstrate the uptake of CO_2 by algae to produce O_2. The idea of this project, developed by Dr. Ariya, then has continued and grown. My work has comprised in developing the photo-bioreactor into a hybrid system by designing and integrating a trap system for the capture of toxic by-products, and which could work using renewable energy.

Table of Contents

List of Figures

List of Tables

1. Introduction

1.1. Air pollution and climate change

Air pollution is a global issue that has increasingly drawn attention over the recent years, as growing evidence demonstrates the adverse impact it has on health and the environment. Epidemiological research has shown that ambient and indoor air pollution can cause respiratory and cardiovascular diseases, among other health-related problems.[1] The World Health Organization (WHO) estimated that 3.7 million premature deaths in 2012 were due to outdoor (ambient) air pollution.[2] Furthermore, air pollution is closely linked to climate change. The emissions of pollutants and unfavourable weather conditions lead to poor air quality, adversely impacting the Earth's climate.

Natural factors and human activities can alter the Earth's energy balance, contributing to climate change. Factors that can affect the Earth's climate include: changes in the sun's energy and in the shape of the Earth's orbit causing variations in the amount of sunlight reaching the Earth's surface; changes in the Earth's reflectivity depending on its surface and atmospheric composition (including clouds); and variations in greenhouse gases (GHGs).[3]

The Sun's incoming radiation to the Earth can be reflected back to space or absorbed by the Earth. According to measurements from the Total Irradiance Monitor (TIM) on NASA's Solar Radiation and Climate Experiment (SORCE), the present total solar irradiance is 1360.8 ± 0.5 W/m^2.[4] How much sunlight is reflected or absorbed is influenced by the planet's surface and atmosphere. Energy, resulting from sunlight absorbed by the Earth, is released back into space by the Earth's surface and atmosphere as infrared radiation (long wave radiation). Greenhouse gases, such as carbon dioxide (CO_2) and methane, can trap this long wave radiation and prevent loss of heat back into space; thus warming the Earth. This is known as the "Greenhouse Effect".[5] Another potent GHG is tropospheric ozone (O_3), a secondary pollutant generated from chemical reactions between volatile organic compounds (VOCs) and carbon monoxide (CO) with nitrogen oxides.[6]

The Earth's albedo at the top of the atmosphere, i.e. the amount of sunlight reflected from the planet's surface and atmosphere (including clouds), is approximately 30 %. Air pollutants can impact radiative forcing. Air-borne particles, i.e. aerosols, impact the planet's energy balance by altering the Earth's reflectivity. They can absorb or reflect solar radiation, depending on their composition.[7] Several aerosols are man-made, such as soot which can have a warming effect on the planet, or sulphate aerosols which have a cooling effect.

Global warming can lead to serious consequences and have significant implications for humans. As temperatures rise, climates are altered in different ways. The atmosphere's capacity of holding water will change, affecting water cycles and precipitation. Extreme events will be more likely to occur and some locations will receive more precipitation while others will become drier, posing a risk to crop productivity from droughts or flooding along rivers or coastal areas. Furthermore, vulnerable ecosystems, such as the Arctic, are at risk due to temperature changes. Over the past years, rising sea levels and melting glaciers are some of the changes that have been observed.[8]

Countries around the globe have acknowledged that climate change is happening and that action must be taken.[9] At the end of last year, the United Nations Conference of Parties 21 (UN COP21) Climate Change Conference brought nations together to set an agreement to combat climate change, set goals for a more sustainable future and reduce greenhouse gas emissions.

One of the main outcomes from UN COP21 was the aim to keep the global temperature rise under 2 °C above pre-industrial levels.[9] Furthermore, the International Panel on Climate Change (IPCC) has suggested immediate action to control the emissions of GHG's, which includes CO_2.[10]

1.2. Carbon dioxide – A major greenhouse gas

Carbon dioxide is one of the main greenhouse gases, which can contribute to global warming. This is a worldwide problem that affects both industrialized and developing nations as the world's population keeps on growing. The increasing amount of anthropogenic carbon dioxide emissions that is released over the years can lead to a rise in global temperatures adversely impacting our climate. Global CO_2 concentrations have risen by 42% since the pre-industrial age and continue to rise with an average growth rate increase of ~2 ppm per year.[11] Figure 1 shows the global averages of atmospheric CO_2 measurements in parts per million by volume (ppmv), which demonstrate that carbon dioxide emissions are still on the rise.[12]

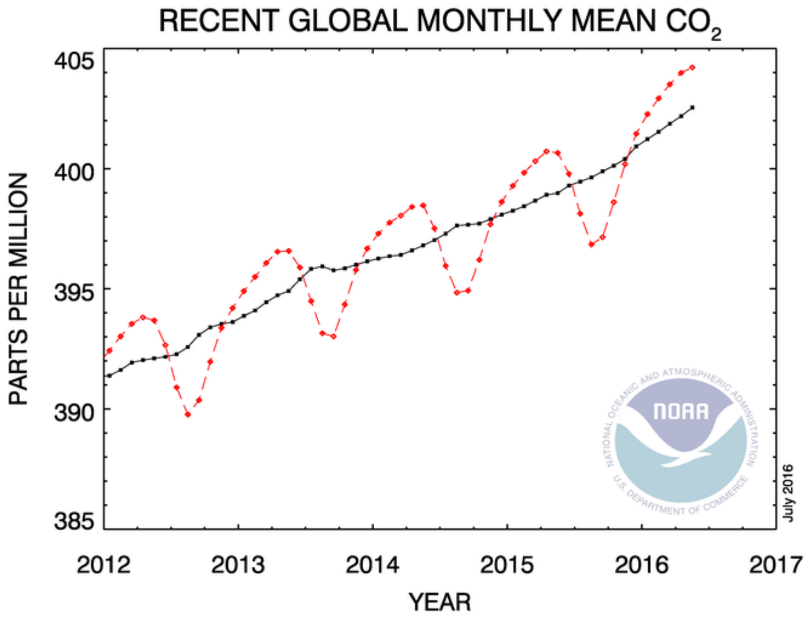

Figure 1. Global Monthly Averages of CO_2. The dashed red line represents the monthly mean atmospheric CO_2 mixing ratios (globally averaged over marine surface sites) and the black line too, but with a correction for the average seasonal cycle.

(Data source: Ed Dlugokencky and Pieter Tans, NOAA/ESRL)[13]

1.2.1. Sources of carbon dioxide in the atmosphere

The energy sector is the largest contributor of global GHGs, and carbon dioxide represents 90 % of these emissions.[14] CO_2 is mainly produced by burning fossil fuels, which is also a major source of several air pollutants. In the United States, almost 70 % of electricity generation comes from fossil fuels.[15] Global CO_2 emissions totaled 32.2 $GtCO_2$ in 2013, and the top ten emitting countries, including China and the United States, were responsible for two thirds of these emissions (21.6 $GtCO_2$). The major sources of anthropogenic CO_2 come from electricity and heat generation, transportation and industrial applications, as presented in Figure 2(a).[14] A significant portion of the CO_2 emitted from the industry sector is due to combustion processes; therefore the development of a sustainable approach to mitigate carbon emissions is of great interest.

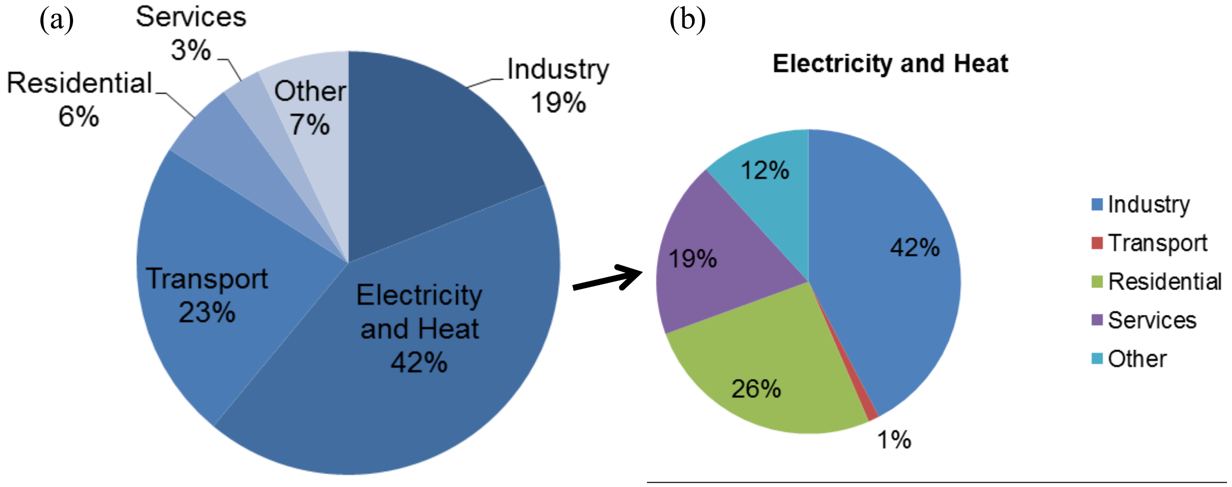

Figure 2. (a) World CO_2 emissions by sector and (b) Sector portions from electricity and heat generation, in 2013

(Data source: IEA Statistics) In Fig. 2(a): "Other" includes emissions not specified elsewhere: agriculture/forestry, fishing, and energy industries other than electricity and heat generation

An effective approach to reduce CO_2 emissions is by limiting the combustion of fossil fuels, such as coal, oil and natural gas. Fossil fuels are non-renewable sources of energy; therefore a move towards renewable energy sources should start playing a greater role in order to rely less on the use of fossil fuels. This would be a desirable long-term goal for the reduction of CO_2 emissions. Yet due to their cost competitiveness compared to other energy sources, it is improbable that fossil fuels will be completely discontinued in the short-term.

1.2.2. Carbon capture technologies

Different approaches can be taken in order to reduce and control the amount of carbon dioxide present in the atmosphere. One way is to use energy more efficiently. Another option is to shift the use of fossil fuels to renewable energies and the use of cleaner fuels, such as biomass fuels. A third alternative is the separation, capture and sequestration of carbon emissions from point-emitting sources.

1.2.3. Carbon Capture and Storage (CCS)

Carbon capture and storage technologies serve as a transitional approach of controlling carbon emissions before shifting away from fossil fuels, while cleaner fuels are further developed and implemented into new and existing plants. Carbon capture can be applied in three different ways: post-combustion carbon capture, pre-combustion carbon capture and oxy-combustion carbon capture.[16-17] Post-combustion capture consists in the separation of CO_2 from the flue gas (mainly composed of a nitrogen-carbon dioxide mixture), whereas pre-combustion carbon capture involves the removal of CO_2 before combustion. Oxy-fuel combustion uses oxygen, instead of air, and recycled CO_2 as the combustion gas.

Oxy-fuel combustion produces flue gas with fewer by-products and a higher concentration of CO_2 which in turn simplifies the CO_2 separation process. One of the challenges with oxy-fuel combustion is the high energy cost to supply oxygen;[17] an air separation unit is usually required to remove the nitrogen and produce a stream of pure oxygen.[16] Some of the limitations of pre-combustion capture are the high costs, and insufficient development work for industrial purposes.[17] Challenges associated to post-combustion capture include added energy requirements for the CO_2 compression step, possible added energy requirements for regeneration of the sorbent used to capture the CO_2, and the need to work with higher volumes of gas due to the lower concentration of CO_2 in the flue gas.[17] Nevertheless, the advantage of post-combustion capture is that it is easier to implement into existing combustion processes, without significant modifications to the plant.

Post-combustion carbon capture technologies include: chemical and physical absorption, chemical adsorption (such as amine scrubbing), and membrane separation. Other options consist of the use of cryogenic processes or carbon adsorption (using molecular sieves). Moreover, the complete chain of CCS technologies involve the sequestration of CO_2 underground such as in depleted oil reservoirs or active oil wells for enhanced oil recovery; or underwater (ocean sequestration).[18] Yet, shortcomings of CCS include high cost, potential leakage back into the atmosphere, or ocean acidification which could damage the marine ecosystem.[19] Furthermore, the potential effects of injecting significant volumes of CO_2 into geological formations are a concern, such as the impact on the quality and flow of water from saline aquifers which still needs further research.[18, 20]

1.3. Photo-bioreactors for CO_2 mitigation and the use of algae

An alternative method is the employment of photo-bioreactors (PBRs) for carbon capture. Algae can be used to convert carbon dioxide (produced from combustion) and water into glucose and oxygen in the presence of visible light. This photosynthetic process is divided in two stages: the light-dependent and light-independent reactions. During the light-dependent stage, visible light radiation is absorbed by chlorophyll to form adenosine triphosphate (ATP) and $NADPH_2$ (a biochemical reductant), accompanied by the oxidation of H_2O to O_2. The ATP and $NADPH_2$ molecules produced in the light-dependent stage are subsequently utilized to reduce CO_2 to carbohydrates in the light-independent reactions thereby completing the overall redox reaction shown in equation 1.[21]

$$6H_2O + 6CO_2 \xrightarrow{Light} C_6H_{12}O_6 + 6O_2 \tag{1}$$

Photo-bioreactors can be divided into open or closed systems. Ponds are an example of open systems, whereas closed systems consist of growing the algae under an enclosed environment, in photo-bioreactors. They can be categorized into tubular PBRs, stirred tank PBRs, flat plate PBRs, hollow fibre membrane PBRs, and airlift photo-bioreactors.[22] Open systems are more cost effective, but usually require large open areas and are susceptible to contamination.[23] Closed systems provide superior control of culture conditions and could potentially offer better mass transfer depending on the type of reactor. Further research is still required to ensure effective algal growth with maximum possible carbon fixation on an industrial scale.[22]

1.3.1. Microalgae and cyanobacteria for CO_2 fixation

There has been significant interest in the deployment of microalgae and cyanobacteria over terrestrial plants due to their rapid growth rates and superior ability to uptake CO_2.[24] Microalgae and cyanobacteria also offer further advantages over other plants: they do not compete over land for crops, and they have demonstrated ability to grow in municipal and industrial wastewaters. Algal studies have demonstrated the removal of nutrients from wastewaters, showing a potential for wastewater treatment.[25] Hence, algae are considered an environmental benign option with several applications, and could be used for CO_2 mitigation to reduce greenhouse gases.

After capturing the carbon dioxide for algal growth, the harvested algae could be further processed to be used as a biofuel source or for the production of other by-products. Algal biomass has been considered for use in biofuels, with high oil contents of 20–80 % lipids on a dry-weight basis.[24] Biofuels derived from microalgae, known as third-generation biofuels, are more attractive than first-generation biofuels (derived mostly from terrestrial crops) and second-generation biofuels (derived from lignocellulosic biomass or agricultural waste), if sustainably produced.[26] They can grow quickly due to their simple cell structure and high photosynthetic efficiencies. Additionally, they can be carbon-neutral sources of energy since the carbon in a biofuel has been previously absorbed from the atmosphere.[27]

The use of carbon from the CO_2 to produce algal biomass and subsequent conversion into algal-based biofuels means that the captured CO_2 from the flue gases will be released back into the atmosphere. Although this occurs, microalgae cultivation combined with CO_2 capture from flue gases has shown an estimated capacity to double the amount of energy produced per unit of CO_2 released.[28]

Microalgae-derived biofuels also offer further environmental advantages compared to fossil fuels which have shown to be unsustainable sources of energy: biofuels are non-toxic and biodegradable. Furthermore, biofuels produced from microalgae serve as a renewable source of energy to replace the depleting reserves of fossil fuels. The burning of fossil fuels post-industrialization has added CO_2 to the atmosphere that was previously trapped beneath the surface of the earth. Shifting to biofuels can conceivably be beneficial as, when sustainably processed, no new CO_2 is emitted into the atmosphere.[27, 29]

Furthermore, the build-up of algal biomass from the PBRs can also be used for other by-products. Algae residue can have commercial value; it can be used as fertilizers for crops or as animal feed.[25] Algal biomass can also be synthesized to produce high-value products such as nutritional supplements, cosmetics and for pharmaceutical applications.[27] A challenge that could arise from the production of algae is generation of toxins and emission of harmful by-products such as volatile organic compounds into the atmosphere. Control of their emissions is a subject that should be addressed.

1.4. Remediation of by-products

1.4.1. Volatile Organic Compounds – Contributing to the Greenhouse Effect

Volatile organic compounds are another important group of air pollutants, released also during stack emissions. The United States Environmental Protection Agency defines them as "*any compound of carbon, excluding carbon monoxide, carbon dioxide, carbonic acid, metallic carbides or carbonates, and ammonium carbonate, which participates in atmospheric photochemical reactions, except those designated by EPA as having negligible photochemical reactivity".*[30] These organic chemicals, which contribute to air pollution, can be emitted from natural or anthropogenic sources. VOCs are of concern both indoors and outdoors, since they can be detrimental to the environment and human health. Therefore, it is of great importance to look into abatement technologies in order to minimize and control their emissions.

1.4.2. Environmental impact

The involvement of volatile organic compounds in the production of organic aerosols, and their role in photochemistry affect the Earth's radiation balance. VOCs are precursors to the formation of tropospheric ozone and particulate matter in the atmosphere, which are the main constituents of the air pollutant known as smog. In the presence of sunlight, many VOCs form ground-level ozone by reacting with molecules that act as sources of oxygen, such as nitrogen oxides (NOx) and carbon monoxide (CO), as shown in the reaction below.[31]

$$NO_x + \boldsymbol{VOC} + Sunlight \rightarrow O_3 + NO_x + Other\ Products \qquad (2)$$

Modelling studies have demonstrated that VOCs have significant influence in tropospheric chemistry, which can impact the oxidative potential of the atmosphere, and lead to alterations in our climate.[32] They can also contribute to depletion of the ozone layer, unpleasant odour, and acid rain; leading to damaging effects on the environment.[33]

1.4.3. Health impact of VOC exposure

Exposure to volatile organic compounds, through inhalation, can cause short-term or long-term health effects on humans, some of which are described in Table 1. Several organic compounds can be toxic or are considered carcinogenic such as benzene. Being exposed to VOC concentrations higher than the acceptable limit can negatively impact health in humans, causing headaches, dizziness, and asthma, among others.[33] Moreover, VOCs lead to the formation of photochemical smog which is considered to be carcinogenic and is known to have serious health effects. Table 1 shows some examples of the harmful effects produced by VOCs.[33]

Table 1. Harmful Effects of VOCs (adapted table from Evuti, 2013)

VOCs	Chemical structure[a]	Boiling pt. (°C)[b]	Harmful environmental and health effects
Benzene	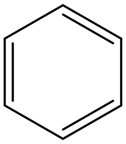	80	Carcinogenic
Toluene	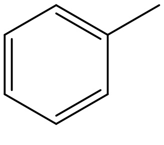	111	Headache and dizziness
Xylene	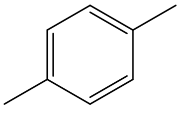	138	Eye and respiratory tract irritation, narcotic effect, nervous system depression

Ethylene, Styrene	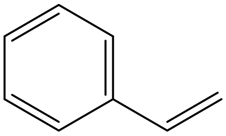 styrene	145	Depletion of ozone layer
Acetaldehyde, Acetone	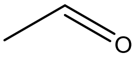 acetaldehyde	20	Respiratory and eye irritation
Phenol	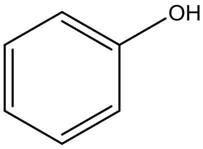	182	Offensive odour and toxicity
Ethers	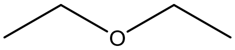	35	Produce peroxides, affect the reproductive system
Vinyl chloride, Freon	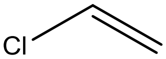 vinyl chloride	-13	Ozone hole formation, carcinogenic, toxic, greenhouse effect, climate changes
Amines (N-containing compounds)	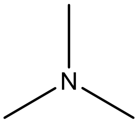 trimethylamine	3	Bad odour, carcinogenic (affect urinary bladder)

[a] Structures drawn with ChemDraw.

[b] Normal boiling points (at 1 atm) shown, obtained from the PubChem database.

1.4.4. Environmental regulations

Strict regulations have been applied over time to control and mitigate the emissions of VOCs, as knowledge of their adverse effects has increased over the years. Environmental standards for the control of VOCs have been implemented around the world. In the United States, VOCs are regulated under the “criteria pollutant” program since they are precursors of ozone. Several compounds have been added to the list since the establishment of the 1990 Clean Air Act and there are usually several others under revision to be included in the list.

In Canada, the provinces and territories (except for Quebec) adopted the Canada Wide Standards for Particulate Matter and Ozone in 2000. It consisted in the reduction of a number of air pollutants including VOCs. In 2003, VOCs were added to the Schedule 1 of Canadian Environmental Protection Act 1999 (CEPA). In 2004, the Ministers of Environment and Health issued a Notice of Intent known as the "Federal Agenda on the Reduction of Emissions of VOC from Consumer and Commercial Products", where it described several measures to be established and applied between 2004 and 2010 in order to decrease the emissions of VOCs from consumer and commercial products.[34] Subsequently, in 2008 the government brought forward regulations to limit these dangerous compounds in architectural and industrial maintenance coatings, automotive refinishing coatings, and selected consumer products.[35] As awareness has augmented, further regulations have been brought to decrease the use of VOCs and mitigate the emissions of these harmful pollutants; hence there is a need to have effective treatment options to remove VOCs.

1.4.5. Sources of VOCs

Volatile organic compounds come from natural and anthropogenic sources. Anthropogenic sources emit about 140 teragrams of carbon per year in the form of VOCs, while biogenic VOCs produce approximately 1150 teragrams of carbon per year with the majority of them being emitted by vegetation.[33, 36] Approximately 90 % of the total emissions of atmospheric VOCs come from terrestrial vegetation, thus biogenic VOCs have significant impact on the Earth's radiation budget.[32] Man-made sources originate from manufacturing and chemical industries, petrochemical industries, and automobile emissions; whereas natural sources include plants, oceans and volcanoes, among others.[31] Figure 3 shows non-methane VOC (NMVOC) emissions from different industry sectors.

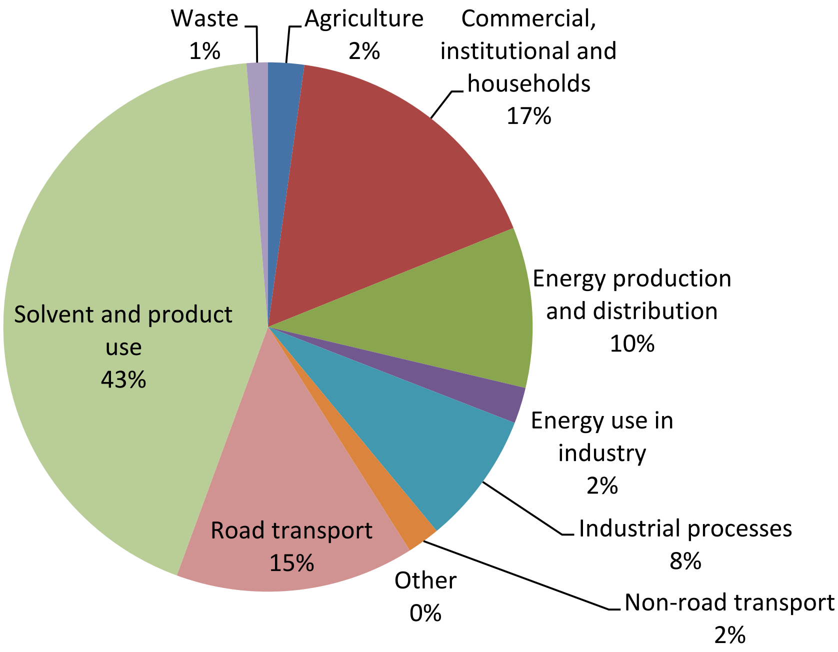

Figure 3. Emissions of NMVOCs from different industry sectors
(Data source: European Environment Agency)[37]

The major anthropogenic sources of concern in Canada come from the oil and gas industry, the use of solvents and its derived products, the transportation sector and from industrial processes. In 2011, the oil and gas industry produced the highest amount of VOCs with a fraction of 31 % (538 kt) of the national emissions, as shown in Figure 4.[38] It should be noted that emissions from natural sources (such as forest fires and volcanoes), and open sources (such as prearranged burning) were not included in the graph. VOCs can be present at very low concentrations (of about 10 ppbv to some ppt), yet they can still have significant effects in the atmosphere.[39]

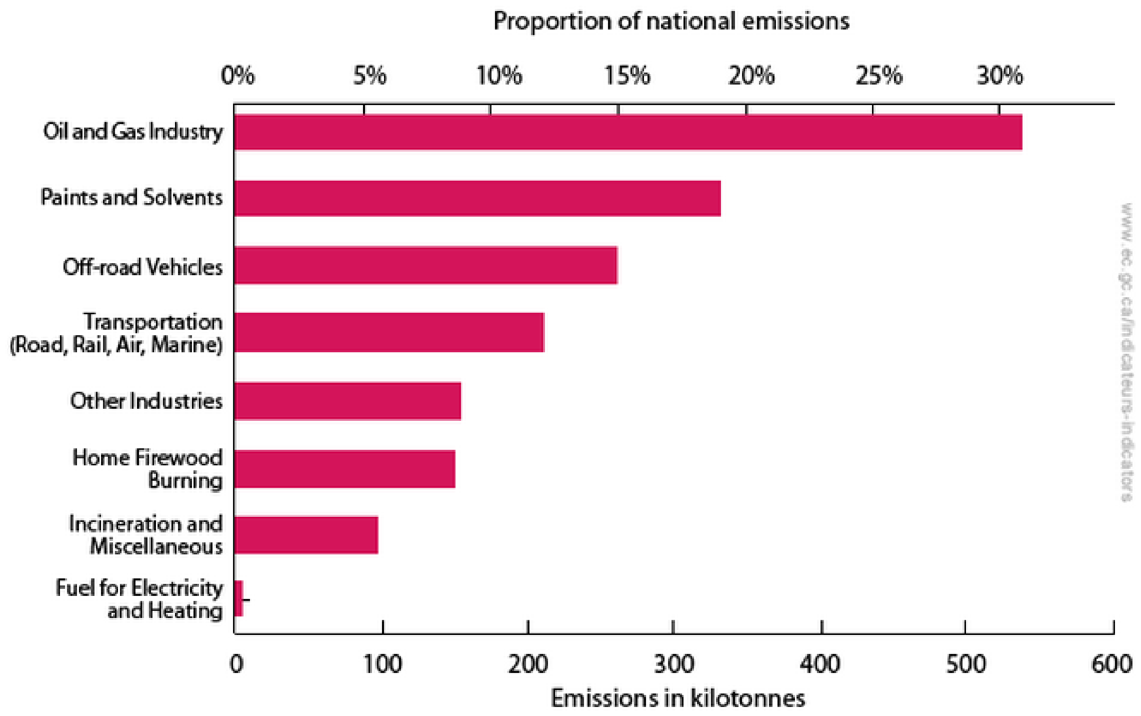

Figure 4. VOC emissions by source, Canada, 2011[38]

As new regulations have been introduced over the years, emissions of VOCs have slowly decreased. In 2011, VOC emissions in Canada were estimated to be 1741 kt, which signified a 4 % decrease from the emissions of the previous year. The latest decrease was mainly due to a reduction of emission levels from the oil and gas sector and the transportation industry. From 1990 to 2011 there was a 29 % (721 kt) reduction in VOC emission levels. The levels were lower due to three main reasons. Firstly, the decrease in emissions from the transportation sector, which was because of the gradual introduction of cleaner technology in the automobile industry. Another factor was from the decrease in emissions from the chemical industries, the petroleum sector and the wood industry. The third reason was from the reduction in VOC usage from products such as paints and solvents.[40] These emissions were only representative of anthropogenic sources. Yet, the largest portion of emissions comes from biogenic sources.

Moreover, combustion processes also contribute to the release of these organic compounds and the implementation of abatement technologies is significant to control harmful emissions.

1.4.6. Overview of remediation technologies

There are several mitigation technologies that exist for the removal of VOCs. However, due to the great variety of VOCs, it is hard to find one unique method. Treatment technologies still require more research to address their limitations and there are also new techniques arising that are still under ongoing research. Several approaches exist to remove VOCs, which are usually classified into changing the process or equipment, or adding control techniques. The treatment technologies can be done by destroying the compounds or recovering them. Some techniques consist in applying chemical, physical or biological processes for the removal of VOCs.

VOCs that are destroyed can be done by oxidation methods such as thermal oxidation, or by bioremediation techniques such as using bio-filters where microorganisms metabolize and degrade the harmful compounds. A wide range of VOCs can be treated biologically. Biological methods are favourable over others in the sense that they usually offer lower capital and operating costs. Some techniques for the recovery of VOCs include condensation, absorption, adsorption, or membrane-based separation. Condensation methods usually have lower removal efficiencies compared to the other techniques and usually demand high maintenance but their recovery product can sometimes counterbalance annual operating costs. Chemical processes like oxidation typically have high removal efficiencies but on occasions they require further control equipment. Absorption and adsorption techniques also offer product recovery which can potentially offset costs; however absorption can require high maintenance and pre-treatment of the VOCs, while adsorption is susceptible to some operating parameters such as moisture or the presence of other compounds which can clog the pores and reduce the efficiency of the process.[31, 41] Figure 5 categorizes the different techniques that can be used for the removal of VOCs.

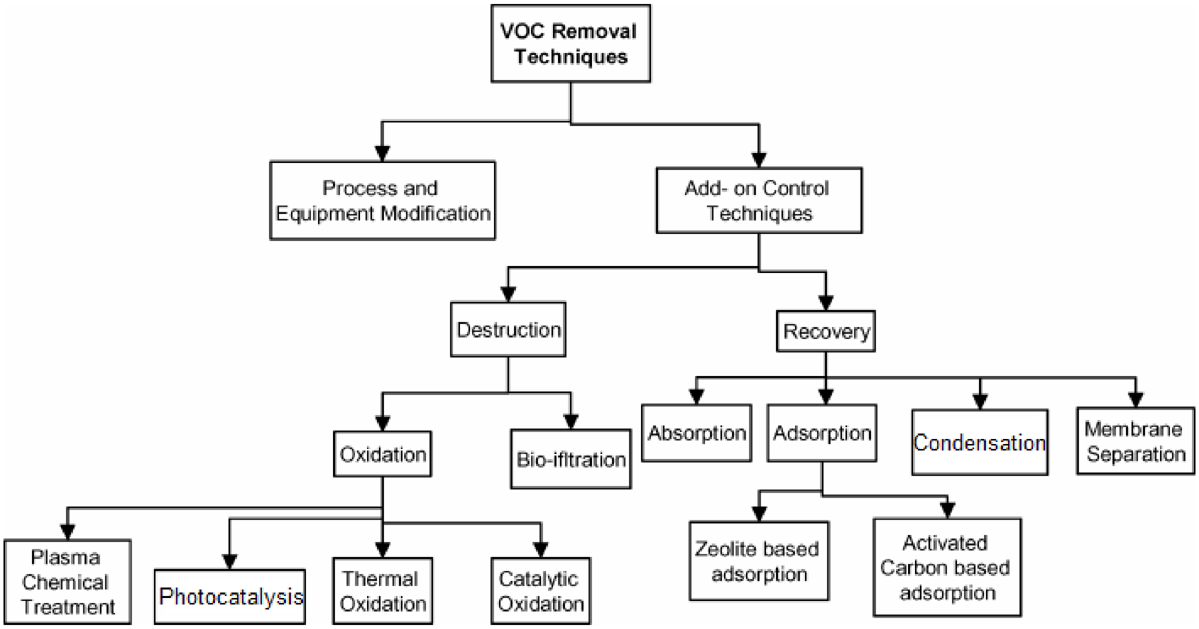

Figure 5. Classification of VOC Removal Techniques[41]

Several approaches, while efficient in the removal of organic compounds, can have an impact on the environment in different ways. Some methods can produce further waste, have high energy requirements, or give rise to other pollutants.[41] Adsorption is one of the leading techniques for removal of VOCs. This approach can be applied to address the problem of controlling harmful emissions that could be released together with CO_2, or produced within algal photo-bioreactors.

1.5. Usage of adsorption interfaces for the removal of VOCs

To treat the by-products, such as semi-volatile and volatile organic compounds, from combustion processes, an adsorption method can be used.

1.5.1. Nano interfaces for remediation of by-products

One of the considerations of employing an algal photo-bioreactor for mitigation of carbon dioxide emissions in combustion processes is the production of by-products and potential release of volatile organic compounds.

The use of nanotechnology has gained popularity over the past few years. One of the fields in which it has received increased attention is in the application of iron nanoparticles for the treatment of environmental pollutants.[42-44]

Nanomaterials are defined as materials having a size of 1-100 nm in at least one dimension and they can be inorganic or carbon based.[45] Nanoparticles present unique properties such as very high specific surface area that has resulted in extensive research being done on their usage for the treatment of contaminants. Their size also permits them to have the rheological ability of flowing into the subsurface and infiltrating crevices where contaminants may be present, and where sometimes even microbes are not available to reach. Examples of such particles include the use of titanium dioxide for the degradation of phenol in wastewater,[46] or research being performed on the usage of carbon-based nanomaterial sorbents for the removal of organic and inorganic contaminants such as divalent metal ions (e.g. Cd^{2+}).[45]

Nanoparticles of zero valent iron (nZVI) are a modification of the well-established technology of using granular and micro-scale iron in permeable reactive barriers for the remediation of contaminated groundwater. This treatment method consists in setting up iron barriers usually supported by gravel beds. The contaminated groundwater is treated as it passes through. Additionally from treating VOCs such as halogenated aliphatics or halogenated aromatics, nZVI can be used to treat pesticides and metals such as arsenic.[47]

Synthesis of iron nanoparticles can be done through several different methods. Some of these include chemical vapour deposition, inert gas condensation, thermal decomposition, thermal reduction of its oxidized compounds, aqueous reduction or iron salts, among others. These methods either consist of producing the nanomaterial from simple building blocks ("bottom up" methods), or they are synthesized through the breakdown of the bulk material into the nanoscale through physical or chemical means ("top down" methods). The most common method of nZVI at a smaller scale is by the reduction of ferric iron with sodium borohydride.[48] Yet iron oxides are naturally occurring in dust aerosols, which make them an inexpensive option as an adsorbent.

The chemistry involved in treating contaminants can be seen in the equations 3-6. The oxidation of iron produces strong reducing conditions where processes such as reductive dechlorination can occur and degrade harmful chlorinated compounds into less hazardous components, leading preferentially to complete reductive dechlorination.[47]

$$2Fe^0(s) + 4H^+(aq) + O_2(aq) \rightarrow 2Fe^{2+}(aq) + 2H_2O(l) \qquad (3)$$

$$Fe^0(s) + 2H_2O(l) \rightarrow Fe^{2+}(aq) + H_2(g) + 2OH^-(aq) \qquad (4)$$

$$4Fe^{2+}(aq) + 4H^+(aq) + O_2(aq) \rightarrow 4Fe^{3+}(aq) + 2H_2O(l) \qquad (5)$$

$$2Fe^{2+}(aq) + 2H_2O(l) \rightarrow 2Fe^{3+}(aq) + H_2(g) + 2OH^-(aq) \qquad (6)$$

Currently, iron nanoparticles are the only "free-released" nanomaterial that has been implemented on a full-scale in the field for remediation of contaminants. Under ambient conditions nZVI can react in water, serving as an electron donor and thus making it a potential environmental remediation material. As seen in Figure 6, they appear to have a core of mostly zero valent iron which is responsible for offering the reducing conditions for the reactions with the contaminants such as VOCs. The shell is mostly iron oxides or hydroxides that result from the oxidation of zero-valent iron and can serve as a surface for chemisorption.[49]

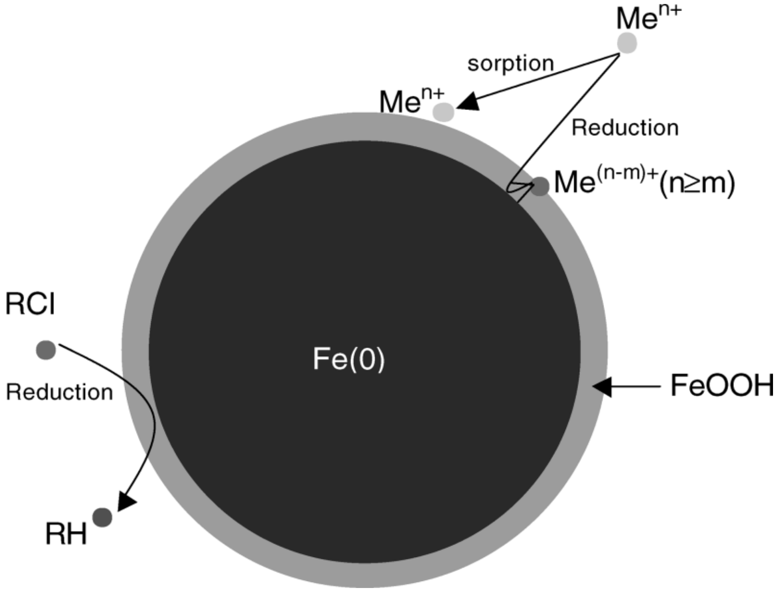

Figure 6. Core-shell Model of nZVI[49]

1.6. Implementation of iron oxides for the removal of VOCs

Iron nanoparticles have been studied for the treatment of contaminated soils and groundwater. Over the past decade, extensive research has been performed on the implementation of iron nanoscale technology, including the application of nZVI for VOC remediation of contaminated soil and water.[50-51] The use of granular iron has been implemented in the permeable reactive barrier technology since the 1990s. It is a well-established method for groundwater remediation that offers low energy costs due to its passive approach, which uses the natural flow of groundwater to pass through the barrier. Iron nanoparticles can be used as a direct modification of this technique, offering further advantages such as higher surface area; which has been found to be correlated with higher reactivity.[47] Additionally, they have also been applied by forming an nZVI suspension and injecting it into aquifers. Nevertheless, further research still needs to be implemented to analyze the remediation potential of iron oxides as an adsorbent in gas streams.

Typical adsorbents used for the treatment of polluted air are zeolites and activated carbon. However, the usage of these adsorbents can generate further toxic waste, such as activated carbon which can produce toxic compounds through oxidations;[52] or they can be expensive, such as zeolite.[41] Significant research has been performed to explore the use of alternate adsorbents. Recent studies have shown that iron oxides, such as magnetite, could serve as a green cost effective adsorbent,[53] due to being a naturally-occurring mineral found in dust aerosols, and its magnetic properties can make it easier to retrieve. Magnetite has been used as a pollutant adsorbent for the removal of arsenic to treat contaminated waters;[54-55] and for the remediation of soils to remove polycyclic aromatic hydrocarbons.[56] Moreover, magnetite particles have been shown to be recyclable, hence reducing waste and offering an inexpensive approach for air pollution remediation.[57]

1.7. Solar energy as a sustainable source of energy

Rising concerns on climate change and air pollution have pushed towards a demand for cleaner and more sustainable technologies. Proposed options include renewable sources of energy such as solar, wind, tidal, biomass, and geothermal.[58-59] One of the most attractive renewable sources is solar energy, an abundant and pollution-free alternative to fossil fuels.[58, 60]

Solar power consists in using the sun's radiation to convert it into electricity. This can be done directly via the use of photovoltaics (PV), or indirectly by using concentrating solar power (CSP).[61] PV's use solar cells to convert direct and diffused sunlight into electricity.[62] CSP uses mirrors to concentrate the sun's radiation that will heat a fluid which will go to a heat engine and part of this heat will be converted into electricity. Some CSP technologies can store the thermal energy to produce electricity at night.[59]

The sun is the most abundant source of energy, however it is an intermittent energy source and not continuously available, thus energy storage methods are required to have continuous energy available. Another option is the use of a hybrid system, such as wind and solar working together, where their differing peak operating times can complement each other.

Table 2. Cost of electricity generation

Type of Solar Power	Electricity Generation Cost ($/kWh)	Location	Year	Reference
PV	20-35	U.S.	2005	58
Thermal (CSP)	15-30	U.S.	2005	
CSP	0.18	North Africa, South America, and Australia	2010	61
	0.12		2030	
	0.11		2050	
PV	0.17	Northern Chile	2010	61
	0.12		2030	
	0.11		2050	

As shown in Table 2, PV and CSP technologies still present a high cost of electricity generation compared to fossil fuel alternatives, which present costs of approximately \$0.05/kWh.[61] While the cost of electricity generation with solar power remains high, fossil fuels will still play a major role. However, with further development of the technology, costs are projected to decrease over the years.

1.8. Scope of my project - Development of a hybrid technology

The aim of my project was to work on the development a hybrid unit; a photo-bioreactor that would be coupled to a nano/micro-traps system, which could be operated using renewable energy, and that could be integrated with combustions processes that are point sources for anthropogenic emissions. Figure 7 illustrates a diagram of the proposed sustainable and hybrid system.

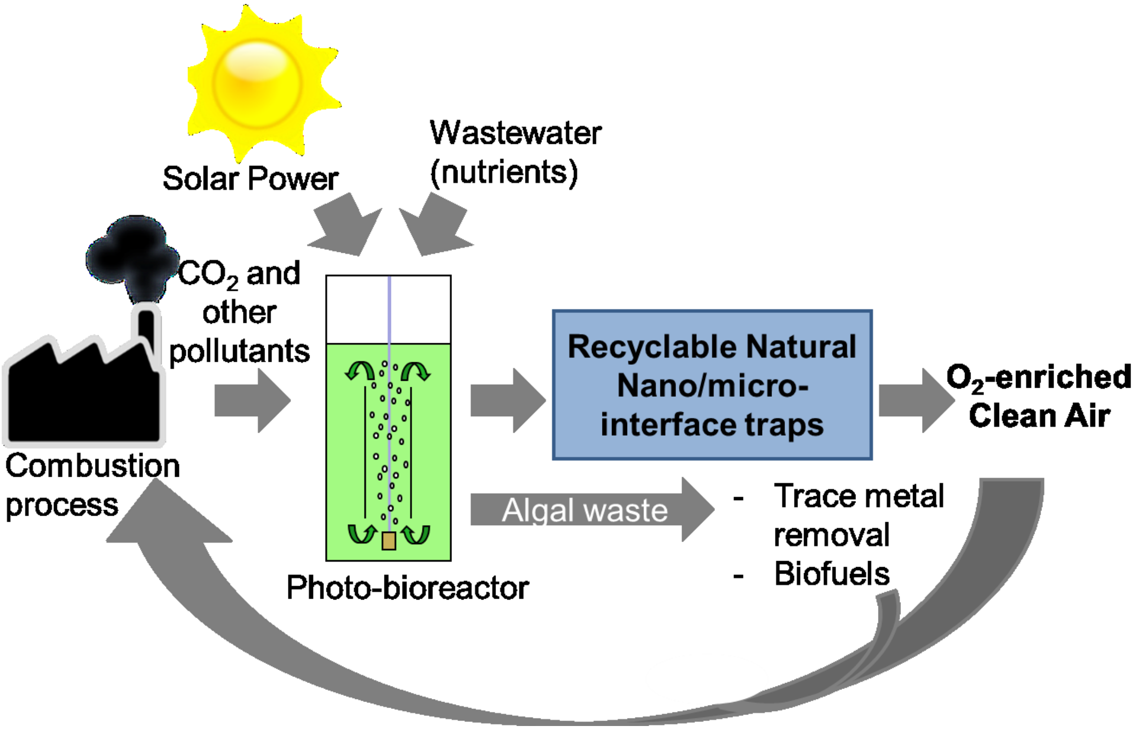

Figure 7. Diagram of the Proposed Sustainable Hybrid Technology

The concept of this technology is to capture air emissions from the flue gas from combustion sources with a green and sustainable approach. As depicted in Figure 7, the system would comprise of an algal photo-bioreactor for the capture of CO_2 emissions directly from combustion sources. One of the objectives was to design a system that would be able to operate at different concentrations of CO_2 relevant to various industrial applications.

The photo-bioreactor unit has demonstrated that it is feasible to produce higher oxygen concentrations in order to obtain a supply of oxygen-enriched air.[63] The production of O_2 would be considered a commodity. The use of oxygen-enriched air back into the combustion process would allow for reduced fossil fuel consumption and increased efficiency in the heating system.[64]

One of my objectives was to look for the presence of VOCs being emitted from the algae, and to design and construct a traps system to connect after the photo-bioreactor unit. The purpose of this setup would be to minimize undesired side-products in the gas stream coming from the reactor, some of which can be harmful compounds. Hence, I used natural-particle traps, which could remove certain volatile and semi-volatile by-products and particulate matter.

Additionally, I examined algae waste that was being produced to use it for further environmental remediation usages. Algae has been studied as an inexpensive bio-sorbent for heavy metals in aqueous systems,[65] for the removal of dyes,[66] and toxic organic pollutants from industrial wastewaters.[67] For this project, I tested its potential to incorporate the algal waste in the system as a sorbent for gaseous co-pollutants that could be present in the air stream, such as mercury, a toxic metal found in flue gas emissions.[68]

The developed design consists of the photo-bioreactor and the nano/micro-traps system coupled to each other; nevertheless it has also been constructed to function independently. I performed various experiments to evaluate its performance, and a feasibility cost analysis to determine its potential up-scaling to different industrial conditions. The system has been designed with a sustainable and green approach, to operate with renewable, environmentally-friendly and cost effective materials.

For my project, in order to control air pollution and global warming issues, and move away from fossil-based sources, I propose the development of a hybrid photo-bioreactor to capture CO_2 and other toxic emissions from flue gas, which could be operable under solar power making it an energy-neutral technology. The developed process consists of two main units: the algal photo-bioreactor and the adsorption trap system.

As a manuscript-based thesis, I have incorporated the paper in the Results and Discussion (section 4) of the thesis. From the manuscript, the Introduction, Experimental and Methodology sections were prepared by me. Dr. Hu contributed with sections 4.2.2 and 4.6.1: the methodology and results on the synthesis and characterization of the iron nanoparticles. Christian Wilde, a previous Master's student, performed work on the photo-bioreactor, some which have been repeated by me. The following sections include the experimental setup and the methodology of the experiments I performed, followed by the manuscript. The cost analysis that I performed is then discussed and I finish with concluding remarks and future work. The project has evolved from a photo-bioreactor to an energy-neutral hybrid system.

2. Experimental Setup

2.1. Algal Photo-bioreactor (PBR)

The first section of the system is an airlift photo-bioreactor. This design consisted of a vertical tube reactor, made of acrylic, with an inner draft tube inside the reactor. The design was chosen by previous student Mr. Wilde. The draft tube was attached to the base of the reactor and had an opening at the bottom to allow for circulation of the fluid, and enhance mass transfer. As illustrated in Figure 8, the inlet tubing for the gas feed was attached to the reactor's lid and placed inside the inner tube (riser section), and had an air sparger connected at the end. The inlet gas stream was passed through the tubing and sparged by the air stone, which created air bubbles for improved mass transfer between the gas and the fluid. The bubbles rose to the top of the inner draft tube, creating an upward motion. Fluid from the outer tube (downcomer section) was drawn in through the inlet at the bottom of the draft tube, creating a downward motion. The gas stream exited the reactor through an outlet tube located on the lid, at the top of the reactor. An O-ring was placed between the reactor and its cap to create a seal at the interface and prevent gases from escaping.

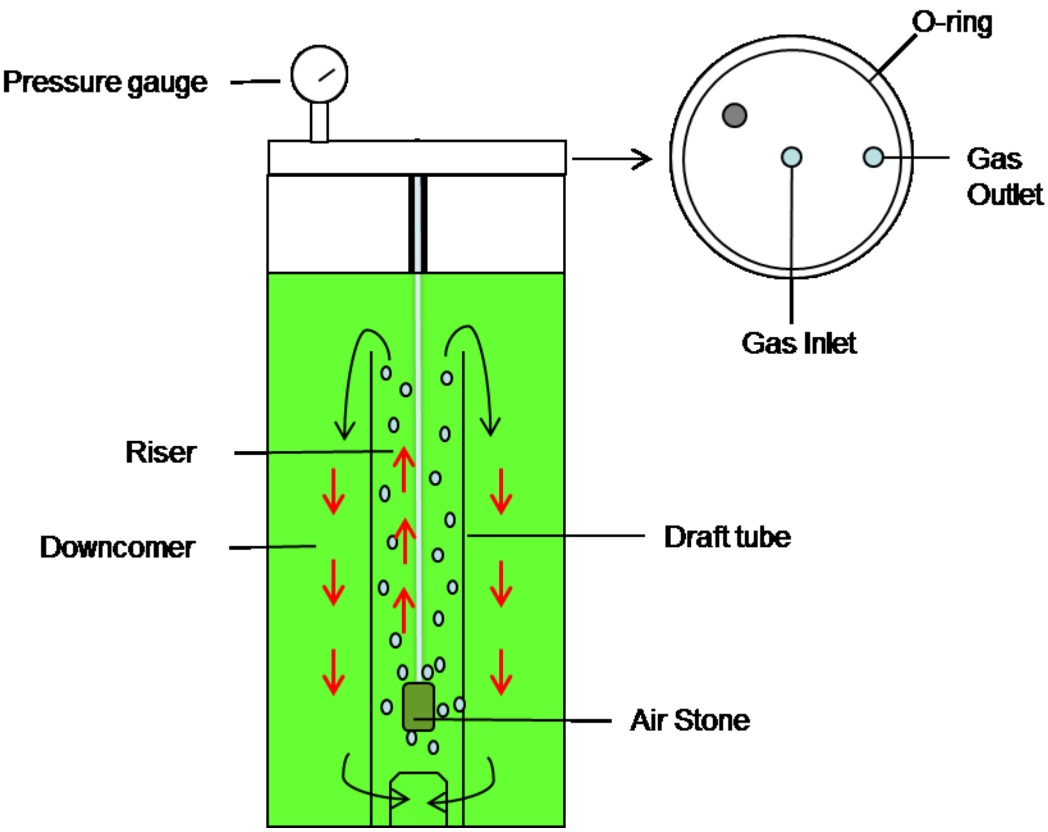

Figure 8. Diagram of airlift photo-bioreactor used for experiments

A quadrilateral casing lined with Polyethylene Terephthalate reflective film surrounded the PBR to support the lights for the reactor. The PBR was illuminated with four Lithonia white fluorescent utility lights (Lithonia Lighting, Model MNS5 2 14 LP, 60 Hz, 28W, length: 54 cm), which were fixed on the casing.

2.2. Nano and Micro-Interface Trap System

The second portion of the set-up is my design: an implementation of a trap system for the remediation of harmful by-products. Two sets of three cylindrical traps, filled with adsorbent particles, were connected in parallel at the outlet gas stream of the photo-bioreactor. As depicted in Figure 9, each line consisted of three stainless steel traps, followed by a particle filter. The first and third traps were packed with 35 g of aluminum oxide microparticles. The middle trap was filled with 2.5 g of nano and micro-size maghemite, and/or 3.5 g of magnetite, packed with untreated glass wool to avoid dispersion of particles into the gas stream, and to allow uniform distribution of nanoparticles without clogging the stream. Untreated glass wool was introduced in both ends of each trap to contain the metal oxides and a 2 μm filter was placed after each trap. The stainless steel cylinders, valves, filters and fittings were purchased from Swagelok.

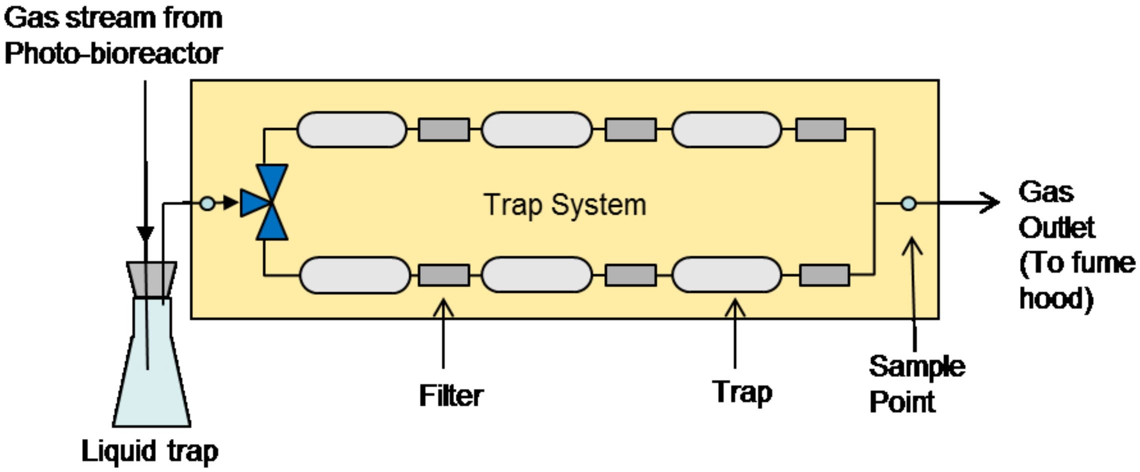

Figure 9. Nano/Micro Interface Trap System coupled to the photo-bioreactor

I designed glass tees, custom-made for the setup, to serve as probe wells. They were placed in-line before and after the trap system for sampling of the gas stream. A liquid/condensation trap was also built using an Erlenmeyer flask and a perforated cap, which was connected between the photo-bioreactor and the trap system. Additionally, O-rings were used to seal the tubing passing through the perforated cap of the liquid trap to ensure an airtight system.

2.3. Overall Schematic of the Hybrid Photo-bioreactor and Trap System Design

Figure 10 shows the flow diagram of the complete set-up. Feed gases were supplied to the photo-bioreactor using pressurized cylinders of N_2, O_2 or compressed air, and CO_2. Filtered room air was also supplied to the PBR via the system pump (from KNF NEUBERGER, model UNMP830 KNDC B). Variable area flow meters (rotameters) from Omega (FL-3861ST), Porter Instruments (B-125-65), and Matheson (R-2-15 AA) were installed to control gas flow rates. Valves and fittings purchased from Swagelok were connected throughout the system to direct the gas flow, for different set-up arrangements.

The PBR-traps system can be adjusted to different flow configurations. The first configuration is the by-pass mode, used for setting up the desired gas mixing ratios and flow rates. This was done by directing the first three-way valve away from the PBR, shown in Figure 10, and sending the flow to the fume hood. The second flow arrangement is the growth mode, to allow biomass density to increase, where the flow from the three-way valve #1 was directed towards the bioreactor and then sent to the fume hood. The third configuration is the remediation mode, which would send the flow through the PBR and subsequently through the trap system. The last arrangement, the recirculation mode, consisted in turning the second three-way valve to direct the PBR outlet flow away from the trap system and back to the pump so it would pass again through the reactor. The purpose of the recirculation mode is for CO_2 capture, for the gas stream to pass through the algal fluid several times to allow an increase in residence time, for improved CO_2 conversion into O_2.

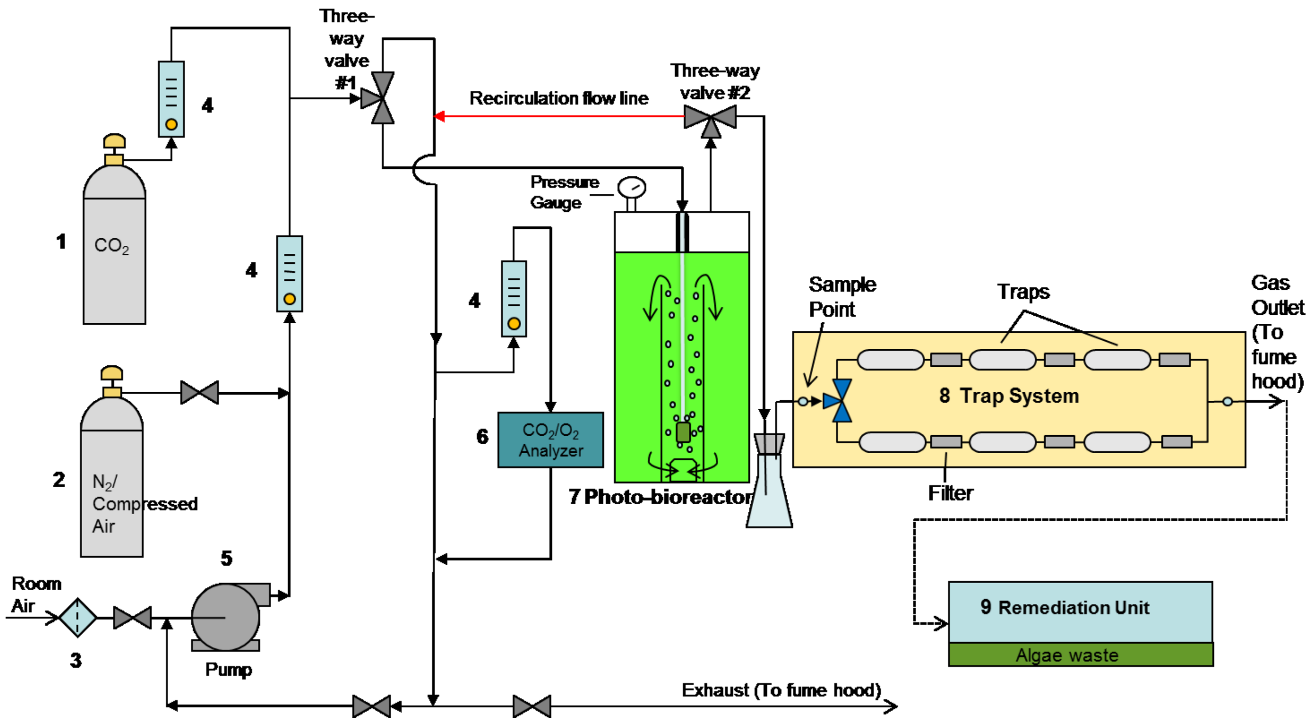

Figure 10. Flow diagram of the experimental PBR-Trap system setup

Table 3. Details of the setup units, corresponding to labels from Figure 10

	Setup parts
1	Carbon Dioxide (99.8%)
2	Nitrogen (99.998%), pre-purified grade; oxygen (99.8%); or compressed gas
3	Filter (Pall TF-1000 PTFE membrane filter: 25 mm, 1.0 mm)
4	Rotameters (from Omega, Porter Instruments and Matheson)
5	Pump (KNF Neuberger UNMP830 KNDC B)
6	O_2/CO_2 analyzer (Quantek 902P)
7	Photo-bioreactor
8	Interface Trap system: composed of three stainless steel traps connected in series, and each trap followed by a 2μm filter from Swagelok. The adsorption interface traps contain metal powders: aluminum oxide, maghemite, and magnetite.
9	Proposed connection of a remediation unit composed of algal waste for removal of co-pollutants from flue gas emissions.

The trap lines were implemented in a parallel configuration to allow for possible continuous removal of the organic by-products. While one set of the adsorbent traps is in use, the adsorbents from the other set of traps can be regenerated and maintained without disruption of the process, permitting continuous operation of the system.

The dashed line in Figure 10 represents a proposed connection to a remediation unit addition to the set-up. The remediation unit would use the algal waste produced from the reactor as a potential remediation interface for gaseous trace metals, such as mercury, a toxic co-pollutant typically present in combustion flue emissions.

3. Materials and Methodology

3.1. Preparation of the Photo-bioreactor setup

3.1.1. Algae cultivation supplies

The nutrients used for algal growth were the following: sodium nitrate, assay 99.0 % min., ACS reagent grade (Anachemia, Montreal, QC); calcium chloride dihydrate, assay ≥ 99 %, ACS reagent grade (ACP, Montreal, QC); magnesium sulphate heptahydrate, assay ≥ 98 %, ACS reagent (Sigma, St. Louis, MO); potassium phosphate powder, assay 99.0 % min., certified ACS (Fisher Scientific, NJ); potassium dihydrogen phosphate, assay 99.99 % (Trace Metals Basis) (Aldrich Chem., Milwaukee, WI); sodium chloride, assay 99.0 % min., certified ACS (Fisher Scientific, NJ); potassium hydroxide pellets, assay ≥ 85.0 % (Fisher Scientific, NJ); iron (II) sulphate heptahydrate, assay ≥ 99.0 %, ACS reagent (Sigma-Aldrich, St. Louis, MO); sulphuric acid, assay 95.0 % - 98.0 %, ACS reagent grade, (ACP, Montreal, QC); boric acid, ACS reagent (Caledon, Georgetown, ON); zinc sulphate heptahydrate, BioReagent (Sigma Aldrich, St. Louis, MO), ethylenediaminetetraacetic acid (EDTA) anhydrous, cell culture tested (Sigma-Aldrich, St. Louis, MO); copper (II) sulphate pentahydrate, assay purity ≥ 98 %, cell culture tested (Sigma-Aldrich, St. Louis, MO), molybdenum (VI) oxide, assay 99.5 % min., ACS (Alfa Aesar, MA). Product specifications were obtained by the manufacturers and all the materials were used as is, without further treatment. Distilled water was used throughout all experiments.

3.1.2. Algae cultivation

Four algal samples were chosen due to their efficient ability to uptake CO_2, which were obtained from Dr. Fussmann and his research team, from the Department of Biology at McGill University. They have previously studied several phytoplankton communities; some of which have demonstrated high resistance to elevated CO_2 concentrations during their growth period and for numerous generations.[69] The species used for evaluation were two green algae species: (a) *Chlamydomonas reinhardtii,* (b) *Scenedesmus sp.* and two cyanobacteria: (c) *Anabaena sp.,* (d) *Synechococcus sp.*

Algae and cyanobacteria cultures were stored in 250 mL Pyrex flasks capped with Kimtech Science Kimwipes, which prevented contamination of the samples but did not block gas exchange with ambient air. All cultures were kept in a container (width: 35 cm, length: 30 cm, height: 24 cm), with the internal walls covered with reflective Polyethylene Terephthalate film along with a compact fluorescent light.

For all experiments the nutrient solution used, for culture growth and storage, was Bold's Basal Medium (BBM).[70-71] Table 4 shows the nutrients, along with their concentrations, used to grow the algae. Algae growth was initiated in the photo-bioreactor by adding ~150 mL of the algae species being tested, to 3.3 L of distilled water with its corresponding volume of BBM

(35 mL of the major stock solutions and 3.5 mL of the minor stock solutions). The algal medium in the PBR was sparged with air to grow at atmospheric conditions (O_2: ~19.2 %, CO_2: 0.1 %). UV-Visible spectroscopy was performed on algae samples taken directly from the PBR using a Varian Cary 50 UV-Visible spectrophotometer before starting experiments, to ensure biomass density would not be a limiting factor. Experiments would start typically after 3-5 days of initial growth of the algae, and by this point the appearance of the medium was green.

The photo-bioreactor was cleaned regularly and to prevent cross-contamination of the different species, it was disinfected every time a different species was used. The PBR, made of acrylic, has a melting point of 160 °C,[72] hence disinfection was done with chlorine and water due to the material of the PBR, instead of using heat. Control tests were performed after disinfection, which showed no algal growth. This was verified by optical microscopy using a microscope (MicroscOptics; model SL-507) with 100X oil immersion objective lens, and a Nikon Coolpix 4500 camera.

Table 4. Components of Bold's Basal Medium (BBM)[73]

Nutrients	Molar Concentration (M)*
6 Major Stock Solutions	
Sodium nitrate	2.94×10^{-3}
Calcium chloride dihydrate	1.70×10^{-4}
Sodium chloride	4.28×10^{-4}
Potassium phosphate	4.31×10^{-4}
Magnesium sulphate heptahydrate	3.04×10^{-4}
Potassium dihydrogen phosphate	1.29×10^{-3}

4 Minor Stock Solutions	
Boron Solution: Boric acid	4.62×10^{-4}
Acidified Iron Stock: Iron (II) sulphate heptahydrate in sulphuric acid	1.79×10^{-5}
Alkaline EDTA solution: EDTA anhydrous	1.71×10^{-4}
Potassium hydroxide	5.53×10^{-4}
Trace metals: Zinc sulphate heptahydrate	3.07×10^{-5}
Copper (II) sulphate pentahydrate	6.29×10^{-6}
Molybdenum (VI) oxide	4.93×10^{-6}

* Uncertainties were not specified.

3.1.3. Set-up of the photo-bioreactor gas feed

CO_2 and nitrogen or compressed air gas tanks were connected to the photo-bioreactor system as seen in Figure 10. During algal growth, filtered room air was supplied to the PBR. Before each experiment was carried out, the feed gas concentrations were measured under the by-pass mode, where the first three-way valve was set to stop the flow towards the PBR and direct gas flow to the fume hood. Feed gas tanks were opened slowly and the CO_2/O_2 analyzer was used to measure the inlet gas concentrations until the desired mixing ratio (with respect to volume) was reached. Once the feed gas concentrations were set, the three-way valve was turned to direct the feed gas to flow to the photo-bioreactor and through the interface trap system, the "remediation mode".

3.2. Algae survival experiments at elevated CO_2 concentrations:

To determine the upper limit of CO_2 concentrations on the algae, each algae species was sparged continuously with different volume mixing ratios of CO_2 in air for a period of time (between one to three days). Algae growth and survival concentrations were determined by visual inspection.

3.3. Characterization of the algal species

3.3.1. Optical microscopy

Optical microscopy was performed on the algal species. With the use of a pipette, a small sample was taken from the photo-bioreactor. The sample was withdrawn from the middle or two thirds down of the photo-bioreactor to ensure that sufficient algae cells were present in the sample when biomass density was limited. Additionally, the walls of the container were roughly scratched with the pipette to release the algae on the wall. Each species was observed and photographed under an optical microscope, using immersion oil and objective lens of 100x.

About 2 drops of the algae sample were dropped on a microscope slide and a coverslip was placed on top carefully, to prevent formation of bubbles. The microscope light was turned on and the sample was subsequently placed under the microscope and focused using the 60x magnification. Using a small tip, such as that of a glass Pasteur pipette, a drop of immersion oil was placed on top of the coverslip and the 100x oil immersion lens was positioned carefully into place. When the lens was in contact with the oil, the microscope was focused until the algae cells were visible. The eyepiece lens and tube were removed and replaced by mounting a camera (a Nikon Coolpix 4500 camera was used) onto the microscope and photographs were taken.

3.3.2. Field Emission Environmental Scanning Electron Microscopy (FE-ESEM)

Field Emission Environmental Scanning Electron Microscopy was also performed on the algae. Algae samples of each species were prepared for imaging by dehydrating them in a graded series of ethanol baths (until 100 %), followed by critical point drying using the Leica Microsystems EM CPD030 critical point dryer. The dried samples were mounted on double-sided carbon tape and coated with a 2 nm layer of platinum coating using the Leica Microsystems EM ACE600 sputter coater. Samples were observed with the FE-ESEM (model FEI Quanta 450) unit and images of each species were obtained.

3.3.3. UV-Visible Spectroscopy

Additionally, the algae were analyzed using UV-visible Spectroscopy at different stages of algal growth. This was performed by filling a quartz cuvette (Hellma Analytics, Type 100-QS) with an algae sample taken directly from the photo-bioreactor. The cuvette was placed in the Varian Cary 50 UV-Visible spectrophotometer and ran under the “Slow” scan mode. Previous to running the algae samples, baseline correction was performed using milliQ water as the baseline. Triplicate runs were performed on the algae samples.

3.4. Solid-phase micro-extraction (SPME) on algae headspace (with and without derivatization)

The formation of organic by-products in the photo-bioreactor from carbon-containing precursors was evaluated. Solid-phase micro-extraction coupled to gas chromatography with mass spectrometry (SPME-GC-MS) was performed to test for the presence of volatile and semi-volatile organic compounds (SVOCs) in the gas-phase overhead.

Two techniques were performed for evaluation of the gas-phase products:

(a) Direct solid-phase micro-extraction (SPME)

(b) Derivatization using O-(2,3,4,5,6-pentafluorobenzyl)-hydroxylamine hydrochloride (PFBHA)

PFBHA is a derivatizing agent that is used for gas chromatography. Equations 7 and 8 show that derivatization with PFBHA produces an oxime which can be detected by the GC.[74-75]

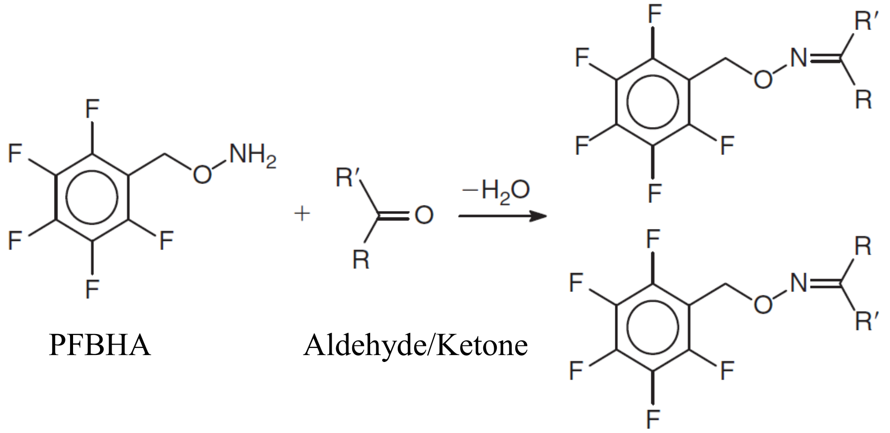

PFBHA

Aldehyde/Ketone

(7)

(8)

Three types of SPME fibres, with different fibre coatings, were chosen to target different functional groups of organic compounds and maximize the VOC/SVOC identification range.[74] The fibres used were: 65 µm Polydimethylsiloxane/Diviniylbenzene (PDMS/DVB), blue; 100 µm PDMS, red; and 75 µm Carboxen/PDMS (CAR/PDMS), black.

Before testing the samples, the fibres were thermally cleaned using the GC-MS to remove any impurity compounds that may have absorbed and accumulated over time onto the fibre. New SPME fibres were thermally conditioned for the first time according to product instructions. Subsequent conditioning was performed by inserting the SPME fibre into the GC-MS injection port for a desorption time of 5 minutes at 250 °C.

3.4.1. (a) Direct SPME analysis

For the direct analysis method, 20 mL of algae were sampled from the PBR and transferred to a small headspace vial, so that it was half-filled with the liquid sample. Consequently, the cleaned SPME needle was carefully inserted in through the septum and into the air-tight vial. Once inserted, the fibre was exposed to the headspace. It was inserted halfway through the vial, close to the liquid sample but without touching it and it was left to absorb the chemicals for 1 hour, with continuous stirring. After the absorption time had passed, the SPME fibre was pulled back into its protective covering, removed from the vial, and transferred to the GC-MS. When injected in the gas chromatograph, the GC-MS run was started with desorption time of 5 minutes at 250 °C, and then the fibre was removed from the inlet. The resulting spectra were then analyzed for compounds to be found in the samples.

3.4.2. (b) Derivatization with PFBHA

For the derivatization method, 20 mL of algae were added to sample vials and additionally 1.22 mg of PFBHA was added to the sample as the derivatizing agent and a magnetic stirrer was introduced. The vial was then capped with a Teflon-faced rubber septum and stirred for 2 hours. The SPME needles were inserted in the gas-tight vials, and the fibres were exposed for 1 hour. Consequently, the fibres were taken to the GC-MS using the same steps as used in the direct analysis method, and the data was collected.

3.5. Imaging of iron oxide microparticles

Field emission environmental scanning electron microscopy was performed on magnetite microparticles. They were placed on an aluminum scanning electron microscopy stub with carbon tape. The magnetite was imaged in the FEI Quanta 450 FE-ESEM at an accelerating voltage of 10 kV using the Everhart-Thornley secondary electron detector at a working distance of 10 mm.

3.6. Preparation of the traps

3.6.1. Preparation of aluminum oxide traps

The first trap of the series was packed with 35 g of aluminum oxide to serve as a drying agent, and avoid water vapour from affecting the iron oxide surfaces. Aluminum oxide pellets (from Sigma-Aldrich) were packed in a stainless steel trap and untreated glass wool was inserted in both ends to contain particles from flowing into the gas stream. The trap was closed with stainless steel connectors, purchased from Swagelok, which were wrapped with Teflon tape.

3.6.2. Preparation of iron oxide traps

The second trap of the set was packed with micro and/or nanoparticle iron oxides to test their ability in removing organic products from the photo-bioreactor gas stream. Depending on the experiment, different iron oxides were used: commercial magnetite (Fe_3O_4) particles from Sigma-Aldrich, synthesized magnetite nanoparticles, and commercial maghemite (γ-Fe_2O_3) nanoparticles purchased from Sigma-Aldrich.

Before packing the traps with the iron oxides, the particles were treated to remove impurities from their surface. Iron oxide particles were placed in a 2 L round glass flask and heated in the oven at 70 °C for 30 minutes. Subsequently, the flask containing the particles was connected to the vacuum line. The particles were flushed with nitrogen using the vacuum line and left under vacuum for 10 minutes, to ensure impurities were desorbed. This process was repeated and particles were flushed three times with nitrogen. Then, the iron oxides were placed in a clean trap, packed with untreated glass wool to ensure containment of particles, and closed with connectors wrapped in Teflon tape. Typically about 2.5 g of nano and micro-size maghemite, and/or 3.5 g of magnetite were used to pack the traps.

3.7. Performance tests on the Trap System

3.7.1. Humidity tests on aluminum oxide traps

Relative humidity was measured before and after the first trap to test the drying capacity of the adsorbent. The photo-bioreactor was connected to the trap system to have the gas stream flow through the traps. Glass tees with their GL-14 cap that were used as sample points in the setup were placed in-line of the gas flow to serve as probe wells, before and after the first trap, which was packed with aluminum oxide. A hygrometer from Aginova (iCelsius wireless with RH probe) was used to insert the relative humidity probe into the probe well and the instrument logged the data with 1-second time resolution.

3.7.2. Trap System: Nano/micro adsorption interface tests

Sample points to analyze the gas stream were placed before and after the trap system using a glass tee with a GL-14 cap and a Teflon-faced rubber septum. A 65 µm Polydimethylsiloxane/Diviniylbenzene (PDMS/DVB) SPME fibre was inserted in the gas-tight glass tee, where the fibre was exposed for 30 minutes and then taken to the GC-MS for collection of the data. Chromatograms from before and after the trap system were then compared to test the adsorption of organic products on the metal oxides used.

3.8. Additional experiments for an energy-neutral closed-loop system

3.8.1. Using renewable solar energy for an energy-neutral system: Solar panel tests

To specify the available power from the photovoltaic module (250W Poly Solar Module, model: CNSDPV250(60)P6-50/45), the working voltage and current of the solar panel were measured using a Fluke 77 Digital Multimeter. Energy requirements of the PBR/interface traps system were measured with an electricity monitor (Kill-A-Watt, model P4400).

3.8.2. Managing algal waste: Absorption tests

To manage the algae waste created from the photo-bioreactor system, I tested the produced algae as a bio-sorbent for the uptake of a toxic compound, elemental gaseous mercury. This was performed using the algal waste produced from the PBR.

Grown algae from the photo-bioreactor were centrifuged to remove the excess liquid. The concentrated algae sludge was placed on a Petri dish and dried in the oven at 60 °C. Dried algae were then crushed with a mortar and pestle.

A 2 L round glass flask was silated, to inactivate the inner surface of the container, and flushed twice with nitrogen, followed by insertion of gaseous elemental mercury into the flask performed by vacuum transfer techniques. 1.2 g of crushed algae were inserted on the side tube; then ran under vacuum and flushed twice with nitrogen, for removal of impurities that could be present. Subsequently, the algae powder was transferred from the side tube into the mercury flask and gas samples from the flask were taken every hour with a syringe and analyzed with the GC-MS.

4. Results and Discussion: Manuscript

The following is a presentation of the paper that I have written that is to be finalized and will be submitted to a peer-reviewed journal. All tests that have just been described in the previous section (Methodology) were carried out by me. For the manuscript: introduction, experimental sections, and methodology were written by me; I have also worked on the results and discussion, unless otherwise stated. Dr. Zhenzhong Hu wrote the segment on the characterization of the iron oxide nanoparticles. The photo-bioreactor section of CO_2 conversion is a contribution from Christian Wilde. Photo-bioreactor work, such as algal survival tests were repeated by me. The paper that I have written is the build-up of the photo-bioreactor to a hybrid green system, where I have implemented a nano/micro traps system, have analyzed the management of the waste of the process and performed a cost analysis.

Development of a Green Hybrid Photo-Bioreactor System coupled with Natural Nano/Micro Recyclable Adsorption Interfaces

Andrea A. Rocha[‡]*, Christian Wilde*[‡]*, Zhenzhong Hu*[†]*, Parisa A. Ariya**[†,‡]

[†]Department of Chemistry and [‡]Department of Atmospheric and Oceanic Sciences

McGill University, 805 Sherbrooke St. W., Montreal, QC, CANADA, H3A 0B9

*Corresponding author: parisa.ariya@mcgill.ca; Tel.: +1 (514) 398 6931

ABSTRACT

We herein report on the development of a novel recyclable bioreactor-oxygen-generation system in concert with iron oxide nano/micro-particle adsorption interfaces, naturally ubiquitous in dust aerosols, to remove CO_2 and undesired compounds, while generating oxygen. Physical and chemical analysis was performed using field emission environmental scanning and high-resolution transmission electron microscopy, UV-Visible and X-ray diffraction spectroscopy, GC-MS, and O_2/CO_2 sensors. A semi-continuous photo-bioreactor system was operated routinely with up to 45 % CO_2 in the input gas stream to the reactor (at a temperature of 34.0 ± 0.5 °C and a pressure of 101 kPa) at the rate of approximately 4 % CO_2 conversion per hour, generating a steady supply of oxygen, while natural nanoparticles remove efficiently several undesired organic by-products, generally formed in bioreactors. The algal waste of the bioreactor was shown to have potential to remove pollutants. This system is found to be recyclable, operable using renewable energy namely solar power, and cost-effective. The implications of the usage of this unit, and potential complementarity to existing industrial setups are discussed.

4.1. Introduction

The International Panel on Climate Change has recommended an immediate decrease in the emission of several anthropogenic greenhouse gases including carbon dioxide.[76] Global CO_2 concentrations have risen by 42 % since the pre-industrial age, and continue to rise.[77-78] The primary anthropogenic source of CO_2 is the combustion of fossil fuels, with major contributors being electricity and heat (41 %), transport (23 %), and industry (20 %).[79] Carbon capture and storage (CCS) has been proposed as a method to mitigate carbon dioxide emissions[19]. It involves CO_2 separation techniques, such as chemical absorption or membrane separation, to remove CO_2 from industrial and energy-related sources. The separated CO_2 is then transported to a durable storage location (e.g. ocean sequestration). Yet, there are major shortcomings with existing techniques such as high operation costs, and potential leakage of CO_2 back into the atmosphere.[80] Moreover, adverse environmental impacts, namely change in the oxidative potential of the atmosphere and interactions with radiation, and formation of unwanted airborne particles, leading to climate change, are also considered.[81-82]

Renewable energy, and process optimizations for improved energy efficiencies have also been deployed to reduce anthropogenic CO_2 emissions limiting the usage of the finite fossil fuel resources.[64] An option that has been studied to capture CO_2 is the use of algae, which can be done in open systems such as ponds or in closed systems.[83] Closed systems consist of growing the algae under an enclosed environment, in photo-bioreactors (PBRs). They can be divided into tubular PBRs, stirred tank PBRs, flat plate PBRs, hollow fibre membrane PBRs, and airlift photo-bioreactors.[22] Open ponds require large areas, and are generally limited to a few algae strains.[23] Culture conditions are often difficult to control and are prone to contamination.[23] PBRs could potentially offer better mass transfer depending on the type of reactor; however, more research needs to be done to cultivate the algae effectively with maximum possible carbon fixation and algal growth, on the industrial scale.[22] Algal PBRs for CO_2 mitigation produce algae that can be harvested for the use of by-products such as biofuel, otherwise it is considered as waste. Notwithstanding the transport of large volumes of gas in industrial setups is energy demanding. Coal power plants are considered to be a primary target of carbon capture technologies, as their flue gas can contain up to ~15 % CO_2.[84] Iron, steel and cement production sectors are also significant targets, as their flue gas emissions include ~30 % CO_2.[85]

Common adsorbents which have been used for the treatment of polluted air includes zeolites and activated carbon.[52] Activated carbon can be flammable or give rise to toxic compounds through oxidation, while zeolite presents higher costs.[41] Due to some of its limitations, recent studies have explored the use of different adsorbents.[86] Some are shown to be very efficient and green in nature,[53] and are used in this study. They include magnetite, a naturally-occurring mineral that has been used for the treatment of contaminated waters[55] and soils,[56] and commonly found in airborne particles, aerosols. Magnetite has been used as a pollutant adsorbent[54] and as a catalyst for redox reactions.[87] Our research group has previously demonstrated that a variety of metal cores including titanium oxides, magnetite and hematite nanoparticles, as well as their composites can adsorb gaseous benzene, toluene, ethylene and o-xylene (BTEX), nitrogen oxides and sulfur oxides, and toxic metals such as mercury.[53, 88-94] We have also shown that used nanoparticles can be recyclable using natural-salt based electrochemistry.[57]

In this paper, we describe the development of a hybrid unit; a green recyclable photo-bioreactor coupled to nano-traps system, which could be operated using renewable energy to run as an energy-neutral system, and that could be easily integrated with combustion processes that are point sources for anthropogenic emissions. The designed system can be operated at different concentrations of CO_2 relevant to various industrial applications and outputs a steady flow of O_2 mimicking photosynthesis by an algal reactor unit. To minimize undesired side-products, the bioreactor is coupled to a system of natural particle traps, which remove certain volatile and semi-volatile by-products and particulate matter, some of which are known as toxins.[95] In our system, we decided to examine the algae waste that was being produced to use it for further environmental remediation usages. It has been studied as an inexpensive bio-sorbent for heavy metals in aqueous systems,[65] for the removal of dyes,[66] and toxic organic pollutants from industrial wastewaters.[67] Here we tested its potential to incorporate the algal waste in the system as a sorbent for gaseous co-pollutants that could be present in the air stream, such as mercury, a toxic metal found in flue gas emissions.[68] The developed design is a multicomponent system that could work individually, or in concert with each other. A large number of sensitivity experiments were performed to evaluate its potential up-scale application to various industrial conditions. The implications of this novel hybrid system in the context of green technology are discussed.

4.2. Experimental Section

4.2.1. Algae preparation

Algal cultures were obtained from the Department of Biology at McGill University. These strains include two green algae species: (a) *Chlamydomonas reinhardtii,* (b) *Scenedesmus sp.)* and two cyanobacteria species*:* (c) *Anabaena sp.,* (d) *Synechococcus sp.* Examples of field emission environmental scanning electron microscopy (FE-ESEM; model FEI Quanta 450) images of these algae are given in the Appendix (p.88), Figure A.1. Algae samples were stored in 250 mL Pyrex flasks plugged with Kimwipes which allowed gas exchange with the atmosphere while preventing contamination. They were kept in a container, with its inside surface covered with reflective PET film (brand: Mylar), along with a compact fluorescent light.

The nutrient solution used for the algae during storage and for all the experiments was Bold's Basal Medium (BBM).[70-71] Algae growth was initiated in the photo-bioreactor by adding ~150 mL of the algae species being tested, to approximately four litres of distilled water with its corresponding volume of BBM. UV-Visible spectroscopy was performed on algae samples taken from the PBR using a Varian Cary 50 UV-Visible spectrophotometer to ensure biomass density would not be a limiting factor during experiments.

The PBR (made of acrylic) was disinfected with chlorine and water, rather than heat due to the low melting point of the acrylic (160 °C).[72] Control tests after disinfection showed no algal growth, verified by optical microscopy using a microscope (MicroscOptics; model SL-507) with 100X oil immersion objective lens, and a Nikon Coolpix 4500 camera.

4.2.2. Synthesis and characterization of iron oxide nanoparticles (NPs)

As described by Massart *et al*,[96] the Fe_3O_4 ($Fe_2O_3.FeO$) NPs were prepared by mixing a 2:1 solution of $FeCl_3{\cdot}6H_2O$ and $FeCl_2{\cdot}4H_2O$ with ammonium hydroxide in 80-90 °C deoxygenated water. The resulting nanoparticles were collected with a magnetic stirring bar and dried in a 50 °C air ventilated oven. The maghemite (γ-Fe_2O_3) mixed nanoparticles were used as purchased from Sigma-Aldrich.

Fe_3O_4 and γ-Fe_2O_3 nanoparticles were characterized with several complementary analytical techniques. X-ray diffraction (XRD) patterns were recorded on a Siemens D5000 diffractometer with Cu Kα radiation source (λ = 1.5418 Å). High resolution transmission electron microscopy (HR-TEM) was taken on a Philips CM200 TEM operating at 200 kV. The

Brunauer-Emmett-Teller (BET) specific surface area (SSA) was analyzed by nitrogen adsorption method on a TriStar 3000 V6.07 surface area analyzer at 77 K.

4.3. Experimental Setup

4.3.1. Photo-bioreactor

A vertical column internal loop photo-bioreactor (PBR) was constructed, as illustrated in Figure 8. Diluent gas was introduced to the PBR through a sparger, suspended within the central draught tube. This design was chosen to enhance mass transfer of the gas into the liquid by creating a pressure difference between inner and outer tubes, forcing the liquid up the central section (riser) and down through the annular outer section (downcomer). Photons were impinged to the reactor using four Lithonia 24" (1"= 2.54 cm) fluorescent lights. The lights were mounted onto a four sided backing covered by a Polyethylene Terephthalate (PET) reflective film (Mylar) that enclosed the reactor.

4.3.2. PBR system setup

Figure 10 (p. 30) shows a simplified schematic of the system setup. It is an airtight system with the exhaust line to the fume hood being the only outlet. Further details of the setup can be found in the Experimental Setup, section 2.3. Pure gases were delivered to the system from pressurized cylinders of CO_2, N_2 and O_2 and filtered room air can also be pulled into the system using the main system pump. Gas flow rates were controlled using variable area flow rotameters obtained from Omega, Porter Instruments, and Matheson. Several valves were placed throughout the system in order to close off the different inlets or outlet, or by-pass sections of the system to obtain different flow configurations.

There are different configurations for the PBR system. For a typical experimental run it usually goes first through a setup period to control mixing ratios of gaseous compounds, then through the growth phase and finally through a recirculation period with a gas flow rate of 0.5 liter per minute (LPM), where the readings are recorded every 10 or 20 minutes, or through the remediation mode depending on the experiment.

The setup mode consists of adjusting the incoming gas flow rates (CO_2 mixed in air, N_2, or O_2) to obtain the desired flow rates and gas compositions. This step is performed while the PBR is offline (i.e. no gas flowing through the bioreactor). Once the targeted flows and targeted compositions are reached, the system is changed to the flushing/growth mode. Here the system flow is diverted so that the reactor is inline. This allows it to receive the incoming gas, pass it through the PBR and release the exhaust gases, through an outlet into the fume hood. The system can remain on flushing (growth) mode for longer periods of time (several days) in order to increase the biomass density, or to test if the algae can survive prolonged sparging with the incoming gas. The remediation mode is similar to the flushing mode but directs the gas flow from the PBR to the traps system, and it then goes to the fume hood. The last configuration is the recirculation mode. After the PBR liquid has reached equilibrium with the gas feed, all system inlets and outlets are closed to obtain a parcel of gas that recirculates continuously throughout the reactor. This is done to approximate the behaviour of a longer reactor, or more accurately, a series of several reactors.

4.3.3. Natural nano/micro trap system

As depicted in Figure 10, a three-trap system was connected in series to the outlet gas stream of the PBR. The first and third stainless steel traps were filled with 35 g of aluminum oxide micro-particles and the middle trap contained 2.5 g of nano and micro-size maghemite, and/or 3.5 g of magnetite, packed with untreated glass wool to avoid dispersion of particles into the gas stream. Untreated glass wool was inserted at both ends of each trap to contain the metal oxides and a 2 μm filter was placed after each trap. The traps and filters were purchased from Swagelok. Several blank tests and a minimum of three repetitions were done for each experiment, to ensure rigorous quality control.

4.4. Methodology for Analysis

4.4.1. Recording data: Mass balance calculation

All experiments, where a change in the gas composition was investigated due to algal activity, were carried out under the recirculation mode. As the parcel of gas was continuously cycled through, a sample was pulled into the analyzer. The pressure from the PBR was recorded along with the CO_2 and O_2 readings. The main system pump was turned off during these readings to ensure the flow did not affect the pressure distribution throughout the system. Otherwise, the pump was on at all times.

The system cannot be operated at a pressure higher than 125 kPa and hence it was periodically vented by opening the outlet of the system. Analyzer and pressure readings were recorded just before and after each venting.

The mass balance of the major constituents (CO_2, O_2, N_2) of the gas over time were calculated since the O_2 and CO_2 readings show the amount of each present in the gas phase at any time, and the pressure in the PBR indicated the total quantity of gas present. The gas that was lost from venting was accounted for by evaluating the change in analyzer and pressure readings. The analyzer readings were normalized to atmospheric pressure in order to report the mixing ratios of each gas. Using this system, no readings could be made of the dissolved gas levels.

4.4.2. Oxygen production rates

Two suggested systems were considered: (I) a semi-continuous oxygen production system, and (II) a batch oxygen-enrichment system.[63] A semi-continuous approach was performed, due to lack of feasible adjustment of inlet and outlet flows of the system that would exactly match the CO_2 consumption and O_2 production rates of the algae. This was achieved by periodically adding pulses of CO_2 to the system, followed by venting the built up gas. The mixing ratio of CO_2 was kept within a certain predetermined range, and the carbon supply in the PBR was never completely exhausted. The "batch oxygen-enrichment system" consisted of flushing the PBR with a gas containing CO_2 so that it would build up in the liquid phase due to its high solubility while the rest of the gases passed through.

4.4.3. Organic product analysis

Solid-phase micro-extraction (SPME) coupled to gas chromatography with mass spectrometry (GC-MS) detection was used for volatile and semi-volatile organic compounds (SVOC) in the gas-phase overhead, to investigate the potential of the formation of organic by-products from primary or secondary carbon-containing precursors within the bioreactor. To maximize the VOC identification range, we employed two methods: (a) direct SPME and (b) derivatization using O-(2,3,4,5,6-pentafluorobenzyl)-hydroxylamine hydrochloride (PFBHA). Details on the PFBHA method are explained in section 3.4.

Three different types of SPME fibres, with different fibre coatings, were used to target different functional groups of organic compounds.[74] The fibres used were: 65 μm

Polydimethylsiloxane/Diviniylbenzene (PDMS/DVB), blue; 100 µm PDMS, red; and 75 µm Carboxen/PDMS (CAR/PDMS), black.

For the direct analysis method, algae samples of 20 mL were taken out from the photo-bioreactor and transferred into a half-filled headspace vial. Before the samples were tested, the fibres were conditioned and thermally cleansed of adsorbed species, in the GC-MS inlet port at 250 °C. Consequently, the cleaned SPME needle was carefully inserted in through the septum and into the air-tight vial. Once inserted, the fibre was exposed to the headspace for 1 hour, with continuous stirring. After the absorption time had passed, the SPME fibre was pulled back into its protective covering, removed from the vial, and transferred to the GC-MS. The exposed fibre was allowed to desorb for 5 minutes at 250 °C, during the analysis, before being removed from the inlet. The resulting spectra were then analyzed for compounds to be found in the samples.

To derivatize the VOCs, 1.22 mg of the derivatizing agent (PFBHA) was added to 20 mL of algae, in a clean sample vial capped with a Teflon-faced rubber septum, and stirred for 2 hours. SPME headspace analysis of the derivatized system was done, using a procedure identical to the direct analysis described before.

4.4.4. Trap system: Nano/micro adsorption interface tests

Sampling ports to analyze the gas stream were constructed before and after the trap system using a glass tee with a GL-14 cap and a Teflon-faced rubber septum. A 65 µm Polydimethylsiloxane/Diviniylbenzene (PDMS/DVB) SPME fibre was used for sampling (with an exposure time of 30 minutes) prior to GC-MS analysis. The data obtained before and after the trap system were compared, to check the efficacy of the metal oxide adsorbents.

4.4.5. Managing algae waste: Absorption tests

To manage the algae waste created from the photo-bioreactor system, we tested the produced algae as a bio-sorbent for the uptake of toxic trace metals, namely mercury, in the gas phase. This was performed using the algae waste, whereby the excess liquid was removed from the harvested algae by centrifugation and dried.

Grown algae from the photo-bioreactor were centrifuged to remove the excess liquid. The concentrated algae sludge was placed on a Petri dish and dried in the oven at 60 °C. Dried algae were then crushed with a mortar and pestle.

A 2 L round glass flask was silated and flushed twice with nitrogen, followed by insertion of gaseous elemental mercury into the flask performed by vacuum transfer techniques. The crushed algae were inserted on the side tube, ran under vacuum and flushed twice with nitrogen. Subsequently, 1.2 g of algae powder was introduced from the side tube into the mercury flask and gas samples were taken every hour with a syringe and analyzed with the GC-MS.

4.5. Materials and Supplies

4.5.1. Algae cultivation nutrients

Algae were cultivated with a Bold's Basal Medium, as described. Detailed information on the nutrients used can be found in Section 3.1.1, Algae Cultivation Supplies. Distilled water was used throughout the experiments.

4.5.2. Organic analysis

Solid-phase micro-extraction (SPME) fibre holders for manual sampling and SPME fibres were obtained from Supelco (Sigma-Aldrich). O-(2,3,4,5,6-pentafluorobenzyl)-hydroxylamine (PFBHA) hydrochloride was purchased from Fluka.

GC-MS experiments were performed on an HP 6890 gas chromatograph, with an HP-5 mass spectrometry column (length: 30 m, internal diameter: 0.25 mm, film: 1.00 µm) purchased from Agilent, which was coupled to an HP 5973 Mass Selective Detector.

4.6. Results and Discussion

4.6.1. Characterization of the Fe_3O_4 and γ-Fe_2O_3 nanoparticles (NPs)

In our laboratory, we have performed extensive physical and chemical studies of metal core nano and micro-particles,[53, 57, 88-90, 92-94] where we focused on fundamental understanding of physical chemistry of gaseous reactions on nano-surfaces, including studied competitive reactions, active sites structure and distribution, and humidity effects.[53, 89] We have also studied the surface adsorption of variety of organic compounds on metal surfaces,[97] and used designed nanoparticles for ultra-trace gaseous measurement.[98] Hence, in this study, we opted to use nanoparticles of naturally occurring materials such as iron oxides to trap unwanted gas phase organic species downstream of the bioreactor.

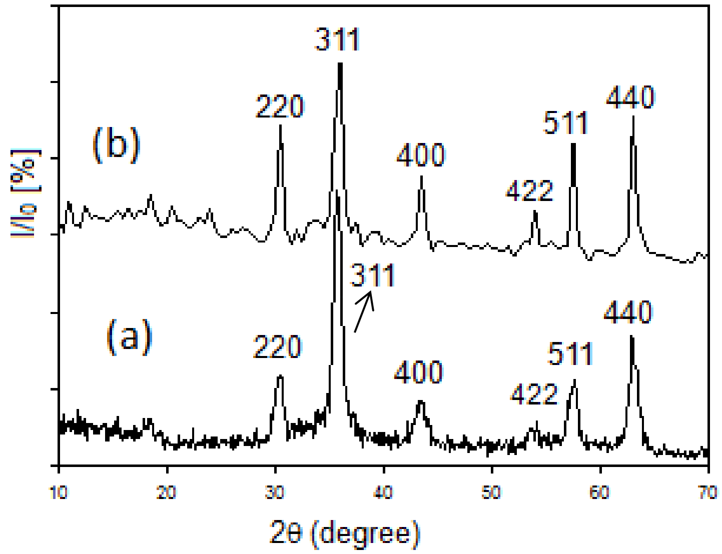

Figure 11. X-ray diffraction patterns of (a) synthesized Fe_3O_4 nanoparticles and (b) commercial γ-Fe_2O_3 nanoparticles

As shown in Figure 11, the XRD relative peak intensities of Fe_3O_4 and γ-Fe_2O_3 nanoparticles matched those of reference Fe_3O_4 (JCPDS card # 19-0629) and γ-Fe_2O_3 (JCPDS card # 39-1346). Figure 11 shows that synthesized magnetite and commercial maghemite nanoparticles have similar crystal structures: Peak 311, shown with an arrow, confirms that the patterns are identical to magnetite and thus confirm the synthesis methods used.[99] The average Scherrer sizes of the Fe_3O_4 and γ-Fe_2O_3 NPs were estimated to be 6.5 and 14.4 nm, respectively. Magnetite and Maghemite have similar crystal structures, and therefore it is difficult to distinguish between them using XRD. The high-resolution TEM images (Figure 12) showed that the synthesized Fe_3O_4 NPs had a narrow size distribution ranged from 8-12 nm. The size of γ-Fe_2O_3 NPs purchased from Sigma-Aldrich had a broad size distribution ranged from 25-125 nm. The BET surface area (SSA) evaluation of Fe_3O_4 and γ-Fe_2O_3 NPs was 84 and 38 m^2/g, respectively.

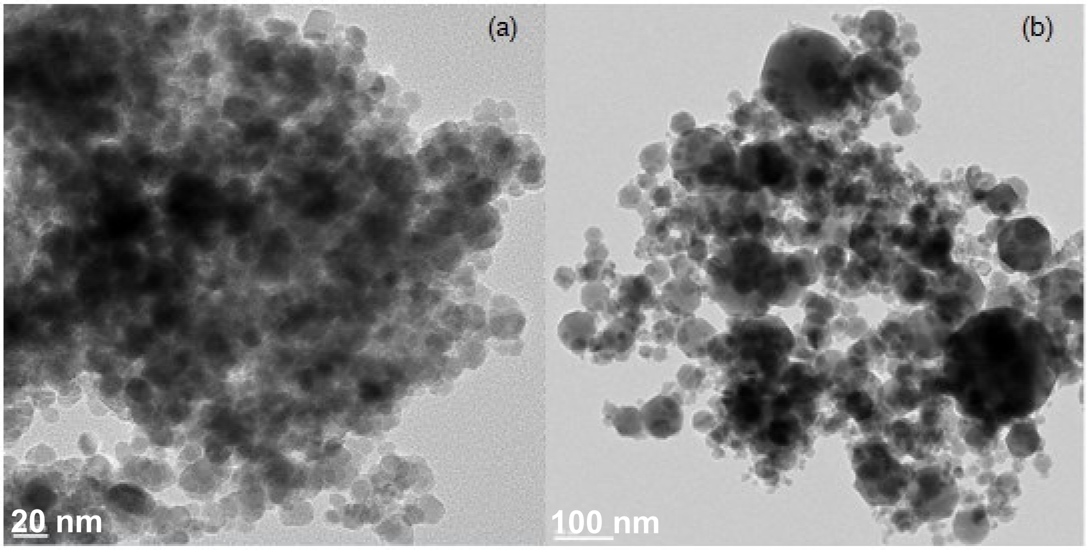

Figure 12. Typical high resolution TEM images of (a) synthesized Fe_3O_4 nanoparticles and (b) commercial γ-Fe_2O_3 nanoparticles

4.6.2. Effect of CO_2 on algal growth, CO_2 consumption and O_2 production

The carbon dioxide consumption and oxygen production rates of *Anabaena sp.* were measured at different CO_2 starting mixing ratios by volume (of 15 %, 30 % and 45 %) in nitrogen, at a temperature of 34.0 ± 0.5 °C and 101 kPa, to test the effect of CO_2 on algal growth. Algae were able to grow in each case and consume approximately all of the CO_2 present, as it can be seen in Figure 13. The oxygen production rates, as shown in Table 5(b), were 6.0 ± 0.2, 5.9 ± 0.2, and 5.7 ± 0.2 mmol/hr for the 15 %, 30 % and 45 % CO_2 starting mixing ratios, respectively. A slight downward trend was exhibited with increasing starting CO_2 concentrations, which could have occurred due to the higher starting CO_2, or possibly due to higher oxygen concentrations experienced during the longer runs, which could have decreased CO_2 utilization for photosynthesis.

Anabaena sp. was able to thrive at a steady rate throughout these experiments even at elevated 45 % CO_2 (in N_2) runs. After a period of 10 hours, the algae went from gas phase conditions of 45 % CO_2, to a gaseous atmosphere of 89 % O_2 and approximately 1 % CO_2. The wide range of oxygen and CO_2 concentrations, used in this study, show that *Anabaena sp.* could be a promising candidate for use in bioreactors operating over multiple oxygen and carbon dioxide concentration ranges.

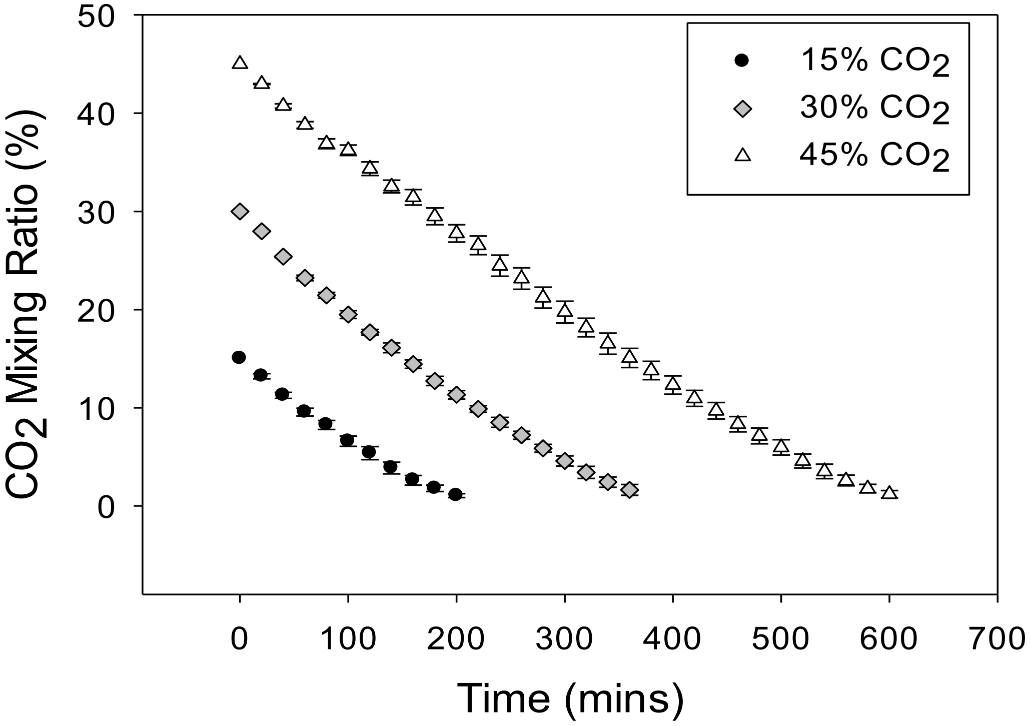

Figure 13. Decrease in CO_2 mixing ratio in the photo-bioreactor containing algae *Anabaena sp.*, as a function of time, at different starting CO_2 (in N_2) concentrations relevant to industrial conditions

4.6.3. Upper CO_2 survival limits

The different species of algae (and cyanobacteria) were sparged with different CO_2 concentrations (mixed in air) to determine their applicable CO_2 ranges at which they can sustain growth. Selected species were not capable of growing above concentrations of 60 % CO_2 in air. In Table 5(b), the maximum concentrations at which the species were able to grow and survive are shown; at concentrations below these ranges, the algae grew uniformly distributed along the photo-bioreactor. The ranges depicted in Table 5 are representative of mixing ratios at which the algae showed continual growth and survived, however at these higher CO_2 mixing ratios the cultivated algae concentrated along the walls of the PBR while the suspension remained clear; indicating that, even though they were not optimal, they are resilient species and can thrive under extreme conditions. Above their respective limits, the species ceased to endure. Studies have demonstrated that some species such as cyanobacteria *Synechococcus* and *Anabaena* can survive higher concentrations of CO_2, up to 100 %, yet only when grown with gradual increments.[100] Hence, one can include the addition of mixing steps with air stream to optimise efficiency for selected industrial applications.

Table 5. (a) Algae survival at different carbon dioxide concentrations. (b) Summary of algae growth experiments at different experimental conditions

(a) Upper survival limits for different algae species

Species	**CO_2 (in air) Mixing Ratio (%)** **Algal survival ranges**
Anabaena sp.	50-60
Synechococcus sp.	10-50
Chlamydomonas reinhardtii	25-60
*Scenedesmus sp.**	50-60

*This strain survived for two days; yet at 60%+ mixing ratios ceased to exhibit any growth.

(b) Algae growth experiments

Species	**Starting CO_2 (%)**	**Diluent Gas**	**CO_2 consumption (%/hr)**	**O_2 production (mmol/hr)**	**O_2 total production (mmol)**	**Final O_2 (%)**
Anabaena sp.	15	N_2	4.2 ± 0.1	6.0 ± 0.2	19.6 ± 0.6	54.2 ± 1.8
Anabaena sp.	15	O_2	3.7 ± 0.2	5.4 ± 0.2	17.7 ± 0.5	-
Anabaena sp.	30	N_2	4.7 ± 0.2	5.9 ± 0.1	34.7 ± 4.6	75.8 ± 3.5
Anabaena sp.	45	N_2	4.5 ± 0.1	5.7 ± 0.1	53.8 ± 0.3	.5 ± 1.1

4.6.4. <u>Comparison of efficiency of different algae species</u>

The growth rate and total oxygen production of the cyanobacteria *Anabaena sp.* and *Synechococcus sp*., and the green algae *Chlamydomonas reinhardtii*, were compared, as shown in Table 5(b). Each species behaved similarly, which suggests that the results of the tests obtained in this study may be applicable to many other types of algae. We observed that an increase in the concentration of carbon dioxide, below the survival threshold value of the algae, only slightly reduced algae growth without other significant effects. Selected algal species, namely *Anabaena sp*., *Chlamydomonas reinhardtii* and *Scenedesmus sp* are capable of surviving across a broad range of CO_2 and oxygen concentrations, and are unaffected by rapid shifts in those concentrations. This information is important to assess the industrially relevant conditions that would allow algae to survive, and also for conceiving entirely new uses for algae in various industrial processes.

4.6.5. Coupling interface to remove undesired Volatile and Semi-volatile Products

a) Efficient nano/micro interface traps

A challenge with algal bioreactors is the emission of volatile organic compounds which form particles in the atmosphere,[95] with adverse climatic and health effects.[101-103] We thus constructed traps of naturally-found nano- and micro-metal oxide particles, which are ubiquitous in dust particles,[104] to remove undesired volatile compounds emitted from bioreactors. All natural traps, composed of pellet aluminum oxides were used to adsorb water, known to deactivate iron oxides particles,[89] followed by another trap containing iron oxides, as depicted in Figure 9. VOCs, once released in air, can affect the oxidative potential of ambient air, and can lead to aerosol formation.[31-32] Moreover some of these compounds, such as dimethyl phthalate and styrene, can be health hazards. Acute exposure to these compounds, via inhalation, can cause eye, nose and throat irritation.[105-106] The use of headspace-SPME-GC-MS was performed to investigate the presence of VOCs. To show the efficiency of the traps, an example chromatogram can be seen in Figure A.4 (See Appendix, p. 92, section 8.3.1), indicating that selected VOCs were present in the algae media, and, as depicted in Figure 14, identified volatile organic compounds were absent upon the usage of our traps, providing evidence that traps can efficiently remove selected volatile compounds including hazardous compounds. Hence we opted for multiple traps system to further remove the residual peaks.

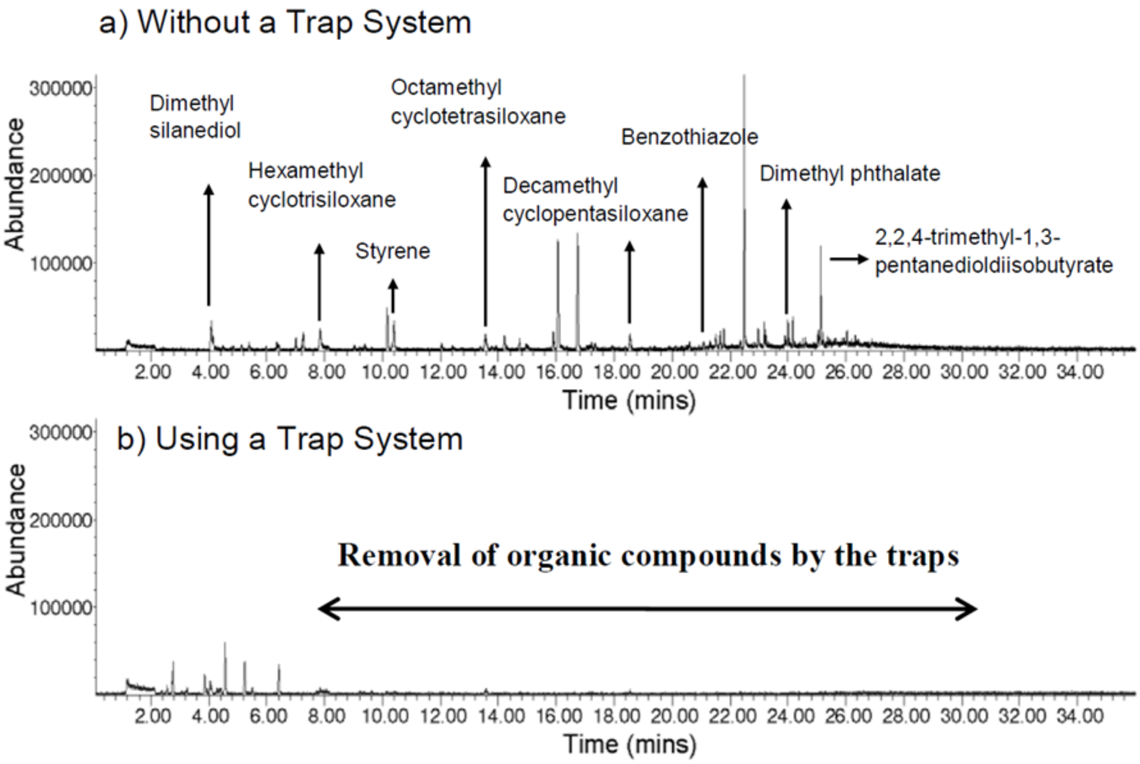

Figure 14. GC-MS Chromatogram samples of a) before and b) after the three-trap system of aluminum oxide, maghemite, aluminum oxide (with 15 % CO_2 in N_2)*

*The earlier peaks appearing below 14 minutes are mostly due to the slight bleeding of GC column.

b) Recyclability of interfaces

In previous studies, several major advances have been made in fundamental understanding of selected surface reactions of certain key atmospheric processes, volatile organic compounds (VOC), NO_x ($NO + NO_2$), SO_2, and water, on nano- and micro- metal oxide and mercury surfaces.[57, 88, 91] Selected organic compounds have been shown to adsorb onto natural nanoaerosol interfaces, including various natural nanoparticles such as those used in this study. The spent nanoparticles can be efficiently regenerated using salt-based electrolysis without loss of their adsorption capacities.[57] The metal oxides used in this study (aluminum oxide, magnetite and maghemite) are components of dust particles in the atmosphere.[53] Magnetite and maghemite are strongly magnetic and thus easy to handle. Furthermore, they can be recycled several times, potentially reducing operating costs of such systems.[57] We paid particular attention to their confinement (with glass wool and filters) to avoid emission of additional aerosols, without preventing air flow circulation.

4.6.6. May the algal waste serve as a remediation interface for pollutants?

Algae have been previously studied for the bio-sorption of heavy metals in aqueous solutions and for the treatment of waste water, demonstrating its potential as an inexpensive sorbent.[107-109] Certain studies have tested the algal biomass without pre-treating it, while other studies have pre-treated the algae as a way to improve their sorption capacity; however some studies showed a decrease in sorption capacity with pre-treatment of the algae.[65]

Mercury is the only liquid metal that has substantial vapour pressure at ambient conditions.[94] Due to its propensity for bioaccumulation, the gaseous mercury can be transported globally, and is considered as a global pollutant. Hence, we performed experiments as a proof of concept to examine whether the algal waste can be served to remove gaseous mercury, which is indeed a co-pollutant in various industrial applications. In this case we performed trial tests using dried algae for the sorption of gaseous elemental mercury, a co-pollutant typically present in stack emissions.

After harvesting the algae for the conversion of CO_2 into O_2, the algae waste, without any other modifications except for drying it, can be reused as an inexpensive bio-sorbent for remediation of trace metals such as mercury. We tested the use of algae waste for absorption of gaseous elemental mercury using the dried algae turned into powder. Under the experimental conditions employed, the mass of mercury absorbed per unit mass of dried algae was found to be 0.92 μg/g (shown in Figure 15). While we performed a pilot study on the potential of waste usage for air stream purification, further targeted research is highly recommended to explore further the potential of the regular waste for decrease of other co-pollutants in the effluent gas emission.

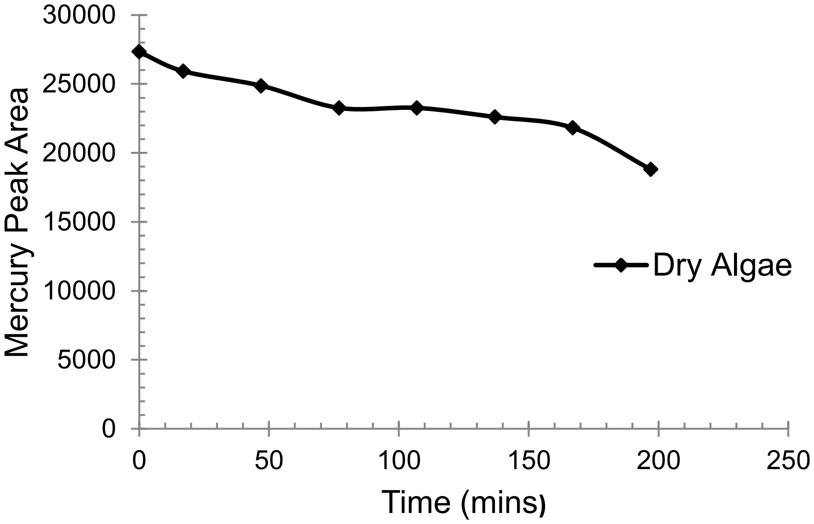

Figure 15. Loss of gaseous elemental mercury with time, in the presence of dry algae

Biosorption of heavy metals is complex and there are limited studies on the recovery of biosorbed pollutants from algae. Recovery of heavy metals such as Pb(II), Cd(II) and Hg(II) sorbed onto algae has been previously achieved by using complexing agents such as EDTA and adjusting reaction conditions (pH, redox potential, etc.); and it was shown that algae can be recycled several times.[110] Proper handling of the toxic algal waste, recovery of Hg(0) and regeneration of the algae may be possible through similar processes, hence further investigation is required. Furthermore, in recent work in our laboratory, it has been shown that the mercury adsorbed on surfaces can be recycled using electrochemistry.[111] The energy used for electrochemical recycling can be supplied from renewable energy sources. Solar energy was shown to be more than sufficient for electrochemical regeneration of mercury.[111] After separation, algae may be reused or utilized for other processes such as the production of biofuels or as a fertilizer, while mercury can be contained or recycled back into industry for further industrial operations.

4.6.7. Could the hybrid system be successful as a CO_2 capture technology and economically feasible?

(a) Success in mitigating CO_2 emissions

Electricity generation relies substantially on coal, the most carbon-intensive fuel, and fossil fuels will still be used while supplies remain. Figure 16 shows the amounts of carbon dioxide emitted in one year using different types of fuels for a typical 500 MW power plant, along with the reduction in emissions if the proposed hybrid photo-bioreactor system would be integrated into the plant, assuming a lower-limit of 30 % CO_2 capture efficiency. Our system demonstrated a capture efficiency of approximately 30 % for a semi-continuous system. However it should be noted that other PBR studies have shown greater reductions in CO_2 concentrations of up to 70 %.[112-114] Valdés et al. demonstrated capture efficiency close to 30 %. This lower value was due to low microalgae cell density, which could also be attributable to our system. As the cell density increased in the PBR, the capture efficiency increased up to a value of 55 %.[112]

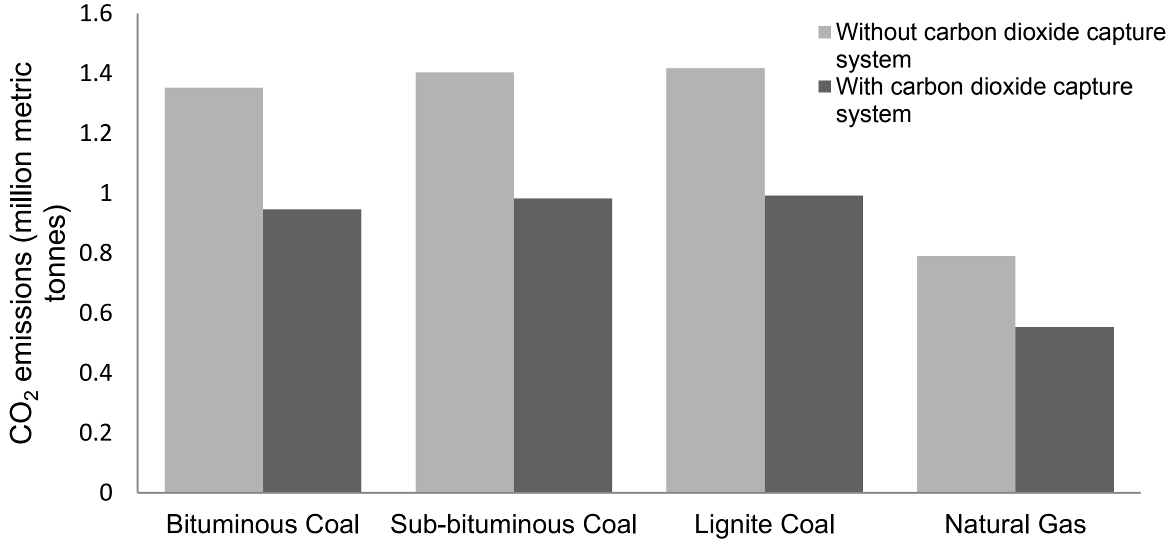

Figure 16. CO_2 emitted per year for a typical 500 MW power plant with different fuels without a CO_2 capture system, and with a 30 % efficient CO_2 capture system

(Fuel CO_2 emission factors were obtained from U.S. Energy Information Administration, 2015)

As fossil fuels remain a major source of fuel, implementing this sustainable capture technology would reduce significant amounts of CO_2 emissions that are released each year. The integration of PBRs in power plants and industrial combustion processes would allow for the connection of a capture technology directly next to CO_2 point sources and reduce substantial amounts of anthropogenic carbon dioxide emissions.

(b) Is the PBR-interface trap system economically feasible?

This hybrid system could be integrated to a CO_2 point source (e.g. coal power plant) without necessarily adding extra energy costs, as energy requirements for this system are relatively low. Furthermore, as opposed to other CCS technologies, the cost of transporting CO_2 through extensive pipelines is not required and hence this lowers the setup costs. The usage of naturally-occurring recyclable nanoparticles, contributes to reductions in operational costs. The next chapter: Cost Analysis, in section 5, discusses in further detail the cost analysis performed on the bench-scale system to evaluate its feasibility for future scale-up.

(c) Incorporating solar energy as a sustainable source of energy

There has been an increasing concern on climate change and air pollution, which has pushed towards the demand for cleaner technologies. Solar power consists in using the sun's radiation to convert it into electricity. It is a pollution-free and renewable source of energy. While solar power technologies still present a high cost of electricity generation (ranging between 0.18 – 35 $/kWh)[58, 61] due to their high capital costs, compared to fossil fuel alternatives which present costs of approximately 0.05 $/kWh, costs are projected to decrease over the years (to 0.12 $/kWh by 2030).[61]

In order to control air pollution and global warming issues, our system is proposed to operate under solar power making it an energy-neutral sustainable technology. We show the solar power availability measured for a solar panel in Figure A.8 (See Appendix, p. 96). The power provided by one photovoltaic module, was sufficient for the energy requirements of the setup, as described in section 8.1. While alternative energy costs remain high, fossil fuels will still play a major role, thus the need still exists to couple this system into existing combustion processes for control of stack emissions.

(d) Environmentally friendly

We opted for the use of inexpensive green materials in order to develop a sustainable system that could reduce CO_2 from flue gas emissions in energy-related and industrial applications, by also limiting the production of toxic by-products and waste. The nanoparticles that were chosen (magnetite and maghemite), that have demonstrated the capture of potential toxic organic compounds from within the system, are not only naturally-occurring but have also been shown to be recyclable using sea salt electrolysis, reducing the amount of potential waste as they can be recycled several times.[57]

The system is proposed to run under renewable energy, namely solar light, to limit production of additional emissions through electricity generation. Additionally, further remediation was tested with the algal waste produced, to examine if it could be potentially used as a bio-sorbent for co-pollutants present in the effluent gas stream, such as mercury emissions and trace metals.

4.7. Conclusions of the manuscript

We herein demonstrated there is potential for up-scaling a hybrid lab-scaled unit, which includes a bioreactor, natural nanoparticle interface, renewable energy and recycling, which removes efficiently carbon dioxide emissions at its source, while minimizing the emission of other co-pollutants. A semi-continuous algal PBR system that converts a stream containing CO_2 to an oxygen-enriched stream is an efficient process, and a fully continuous algal operating system is feasible. Continuous, and not batch, processes are favourable in large-scale applications; yet both techniques may be industrially relevant depending on the other coupled processes. Increased availability of inexpensive oxygen would encourage its use in combustion processes as a replacement for air, and allow for cleaner and more efficient energy production.[115] The coupling of bioreactors with other combustion processes may serve as a hybrid technology, which also reduces atmospheric carbon dioxide emissions.

We have also shown that green natural particle traps can reduce the gaseous emission of undesired by-products significantly. Harvested algae have previously been demonstrated as a biofuel resource.[116] Further studies are recommended on the biological waste from the reactors, as well as to identify the production and reduction of possible pollutants such as VOCs, NO_x, or bioaerosols that are known to affect the environment and human health. Moreover, further analysis of the liquid phase and biomass itself will shed light on the composition of the algae, and the quantity of carbon that is actually being sequestered within the biomass, at different experimental conditions, while providing predictive tools for further optimization of a bioreactor-micro/nano trap system. Knowing the composition of the algae and the ultimate fate of the carbon in the system would allow for a more complete assessment of the carbon capture and biofuel production potential of this process.

5. Cost Analysis to evaluate the potential for up-scaling

5.1. Cost estimate of the hybrid system

An order-of-magnitude cost estimate was performed on the laboratory-scale system to determine the feasibility potential of the design. The energy usage of the design was measured using an electricity monitor (Kill-A-Watt, model P4400) and an average industrial electricity price of 7.96 ¢/kWh was used.[117] It was assumed that the lab-scale system would work 20 hours per day, 5 times a week and 48 weeks per year. With these assumptions, the energy usage for the bench-scale design was calculated to be approximately $45 per year. The nano- and microparticle metal oxides used for the trap system were calculated to cost about $20 per year. Additionally, they have been demonstrated that they can be regenerated several times with an electrochemical chamber, that has been considered to operate under solar energy.[57] Hence, the costs associated with the usage of recycled metal oxide particles were also considered, estimated to be $4 per year for the bench-scale photo-bioreactor system. The system is projected to operate using solar power, so the usage of solar pumps was included in the cost analysis, which decreased the operating costs. The cost of a solar vacuum pump can range between $450 and $520 for the small-scale unit (e.g. brand Goorui). Table 6 shows a summary of these costs.

For the operating cost estimations, market values and industrial prices were used for electricity, water,[118] and oxygen, to evaluate its up-scaling potential. The laboratory photo-bioreactor has been demonstrated to have an O_2 production rate of 6 mmol/hr.[63] It was calculated to produce 922 g of O_2/year, for the assumed time that the PBR would be running in a year. Using an oxygen cost of 0.22 $/kg[119] and the calculated O_2 production rate of the PBR system, the cost of oxygen generated would be 0.20 $/year. This O_2 price, intended as a commodity, was deducted from the yearly operational costs. The analysis was based on a starting concentration of 15 % CO_2, with a CO_2 consumption of 4.2 %/hr that outputs a gas stream composed of 55 % O_2. A higher starting concentration of 45 % CO_2 has been shown to produce a purer oxygen stream (~88 %) which produces similar O_2 production rates (5.7 mmol/hr),[63] and would lead to reduced costs per kilogram of CO_2 removed.

Two scenarios were evaluated in the cost analysis: scenario 1, which consisted of the laboratory design; and scenario 2, which consisted of the proposed system, if the process would be operating with solar energy and with recycling of the nanoparticles. As seen in Table 6, which shows a summary of the estimated costs, the system can be economical when operating with renewable solar energy and with the regeneration of the nanoparticles. It should be noted that for the calculation of the algal nutrients, a high-cost nutrient medium was used for the estimate, using laboratory grade chemicals.

Table 6. Summary of Costs for the Lab-Scale Design

Costs For 1st Year	**Scenario 1 Approximate estimates (in $CAD)**	**Scenario 2 Approximate estimates in (in $CAD)**
Total Purchase Cost	2200	2400 (regular pump replaced with solar pump - $520)
Operating Costs (consumables: metal oxides, algae nutrients)	150	140
Water Cost [a]	0.24	Same as scenario 1
Electricity consumption [b]	45	0
Cost of Oxygen produced per year [c]	0.21	Same as scenario 1
Total Cost for Year 1*	**2400**	**2600**

Costs For 2nd Year and onwards	**Scenario 1**	**Scenario 2**
Operating Costs (consumables: metal oxides, algae nutrients)	150	140
Water Cost	0.24	Same as scenario 1
Electricity consumption	45	0
Maintenance Costs (assumed 10% contingency of operating costs)	20	14
Cost of Oxygen produced per year	0.21	Same as scenario 1
Total Cost for Year 2+ *	**220**	**150**

Data used in calculations:

[a] Industrial water rate of 2.24 $/m^3 (2015 Water Rates, City of Toronto)

[b] 2014 electricity industrial price of 7.96 ¢/kWh (Key Canadian Electricity Statistics, 2014)

[c] cost of oxygen of 0.2 US$/kg O_2, obtained from Eco Global Fuels, USA. Exchange rate used: 1 CAD = 0.89 USD

* Totals may not add up due to rounding

The total purchase costs for the first year were estimated to be about $2160 for the laboratory-scale design, resulting in a total cost of about $2400 for year one, without using solar light and without nano/micro-particle recycling (scenario 1). Installation costs were not included in the assessment. For the second year and onwards, only operating costs of the system were considered (no one-time purchase costs); and a 10% contingency cost of the total estimated operating costs (consumables, water, energy used) was included to account for maintenance costs. This resulted in estimated yearly operating costs of $200 for scenario 1, as opposed to $150 per year for the small scale system when using solar light and nanoparticle regeneration (scenario 2). The total costs for the first year for scenario 2 was greater (~$2600) as a conservative upper limit price for the solar pump was used here.

5.2. Economic potential of the design

The yearly operating and maintenance rates were used to estimate the cost for the removal of CO_2. For scenario 1 the cost was 20 $/kg of CO_2 removed and for scenario 2 (using solar energy and electrochemical recycling of adsorbents) it was about 14 $/kg of CO_2 removed. Algal culture costs were calculated using high-purity grade nutrients, nevertheless algae can be grown in wastewater to cover nutrient requirements,[120] and the annual operating costs would be reduced, resulting in a cost of approximately 7 $/kg of CO_2 removed (scenario 1) and 0.4 $/kg of CO_2 removed for the proposed system (scenario 2).

Energy requirements for the PBR-interface trap system are relatively low. The system could be integrated to a CO_2 point source, such as downstream of many refinery and industrial emissions, without significantly adding energy costs to the process. One of the largest costs for CCS methods is the separation of CO_2,[16] so algal photo-bioreactors are an alternative method which eliminates this step. Furthermore, as opposed to other carbon capture (CCS) technologies, the price of transporting CO_2 through extensive pipelines for its sequestration is not required and hence this lowers the setup costs. The usage of naturally-occurring, recyclable nanoparticles contributes to reductions in operational costs while offering a green approach at capturing other harmful gaseous compounds.

Studies have shown that CO_2 removal from carbon capture and storage technologies can range between 45-150 $/tonne of CO_2 avoided (US dollars),[121] yet they are expected to increase energy costs by 21–91% for existing plants.[19] Furthermore, several cost estimates do not entirely consider site characterization costs.[122] This system offers competitive potential for existing industrial setups, which could be far away from sequestration sites. Thus, the cost estimate performed on the bench-scale system shows that the PBR-interface trap system has potential for further development. It is still projected to be cost efficient in removing CO_2 and toxic by-products, while the waste generated could also be transformed into value added products. Further progress of the technology is still required which would reduce costs as the process evolves, and considering the operating and maintenance costs, future scale-up could be feasible.

6. Concluding remarks and future work

- The designed photo-bioreactor/interface-trap system demonstrated a reduction of organic by-products at the source while reducing CO_2 emissions and producing an oxygen-enriched stream of air.
- The increased availability of oxygen produced in the gas stream could be used to send back to combustion processes, and would allow for cleaner and more efficient energy production. Hence this system is proposed to be coupled to industrial applications to be used as a hybrid technology, without major modifications required for the existing setups.
- The resilient cyanobacteria and microalgae used demonstrated they can thrive under typical CO_2 concentrations found in flue gas emissions.
- The algae could be grown with wastewater, the system could operate on solar power and it was shown that the algal waste produced could serve as an inexpensive biosorbent for the remediation of co-pollutants found in stack emissions, such as mercury.

- The usage of naturally-occurring recyclable metal oxides provided a green and cost-effective approach for the capture of organic by-products.
- The cost analysis demonstrated that the system, with further development, has potential for scale-up and could become competitive against other existing techniques.

Further work into the application of an algal photo-bioreactor as an efficient means to sequester carbon dioxide, and remove resulting by-products, from industrial flue gas is needed before implementation in a larger setting. To accurately assess the possibility to scale a PBR-interface trap system for industrial use it is necessary to model the consumption rates of injected gas and production rates of O_2 at a supposed industrial level. A reliable method to predict output could be possible, as long as models to accurately depict the parameters of CO_2 gas consumption, O_2 content, biomass concentration, saturation limits, among others, are developed.

It is essential to understand the chemical production in the photo-bioreactor to accurately understand a potential implementation of oxygen-enriched air back to the combustion process. Further targeted research is still required to assess the capabilities of nanoparticle interfaces for the removal of organic products from the effluent gas. Furthermore, it is recommended to perform extensive research on the management of algal waste, and further targeted studies on its potential as a biosorbent for gaseous trace metals.

Finally, this system was developed with a green and sustainable approach choosing environmentally friendly methods to mitigate air pollution emissions, while trying to create a closed-loop process to minimize waste and resources. The design is a hybrid multicomponent setup; however each unit could operate independently for different industrial applications.

7. References

1. Rao, S.; Pachauri, S.; Dentener, F.; Kinney, P.; Klimont, Z.; Riahi, K.; Schoepp, W., Better air for better health: Forging synergies in policies for energy access, climate change and air pollution. *Global Environmental Change* **2013,** *23* (5), 1122-1130.

2. Organization, W. H., 7 million premature deaths annually linked to air pollution. *World Health Organization* **2014**.

3. Melillo, J. M.; Richmond, T.; Yohe, G. W., Climate change impacts in the United States: the third national climate assessment. *US Global change research program* **2014,** *841*.

4. Kopp, G.; Lean, J. L., A new, lower value of total solar irradiance: Evidence and climate significance. *Geophysical Research Letters* **2011,** *38* (1), n/a-n/a.

5. Ramanathan, V.; Feng, Y., Air pollution, greenhouse gases and climate change: Global and regional perspectives. *Atmospheric Environment* **2009,** *43* (1), 37-50.

6. Jacob, D. J.; Winner, D. A., Effect of climate change on air quality. *Atmospheric Environment* **2009,** *43* (1), 51-63.

7. Bytnerowicz, A.; Omasa, K.; Paoletti, E., Integrated effects of air pollution and climate change on forests: A northern hemisphere perspective. *Environmental Pollution* **2007,** *147* (3), 438-445.

8. Rosenberg, N. J.; Epstein, D. J.; Wang, D.; Vail, L.; Srinivasan, R.; Arnold, J. G., Possible Impacts of Global Warming on the Hydrology of the Ogallala Aquifer Region. *Climatic Change 42* (4), 677-692.

9. Cozier, M., The UN COP21 Climate Change Conference and the role of CCS. *Greenhouse Gases: Science and Technology* **2015,** *5* (6), 697-700.

10. Pachauri, R. K.; Allen, M.; Barros, V.; Broome, J.; Cramer, W.; Christ, R.; Church, J.; Clarke, L.; Dahe, Q.; Dasgupta, P., Climate Change 2014: Synthesis Report. Contribution of Working Groups I, II and III to the Fifth Assessment Report of the Intergovernmental Panel on Climate Change. **2014**.

11. Stocker, T.; Qin, D.; Plattner, G.; Tignor, M.; Allen, S.; Boschung, J.; Nauels, A.; Xia, Y.; Bex, B.; Midgley, B., IPCC, 2013: climate change 2013: the physical science basis.

Contribution of working group I to the fifth assessment report of the intergovernmental panel on climate change. **2013**.

12. Dlugokencky, E.; Tans, P., Trends in atmospheric carbon dioxide. *Avaiable from: http://www. esrl. noaa. gov/gmd/ccgg/trends. Access in* **2013,** *25*.

13. Tans, E. D. a. P. www.esrl.noaa.gov/gmd/ccgg/trends/ (accessed July 2016).

14. Van der Hoeven, M., CO2 emissions from fuel combustion–highlights. *IEA Statistics* **2015**.

15. EIA, U., Monthly Energy Review, January 2015. US Energy Information Administration, Washington, DC. http://www. eia. gov/totalenergy/data/monthly: 2015.

16. Hills, T.; Leeson, D.; Florin, N.; Fennell, P., Carbon Capture in the Cement Industry: Technologies, Progress, and Retrofitting. *Environmental Science & Technology* **2016,** *50* (1), 368-377.

17. Ben-Mansour, R.; Habib, M. A.; Bamidele, O. E.; Basha, M.; Qasem, N. A. A.; Peedikakkal, A.; Laoui, T.; Ali, M., Carbon capture by physical adsorption: Materials, experimental investigations and numerical modeling and simulations – A review. *Applied Energy* **2016,** *161*, 225-255.

18. Rubin, E. S. In *IPCC Special Report on Carbon Dioxide Capture and Storage*, RITE International Workshop on CO2 Geological Storage, Tokyo, Tokyo, 2006.

19. Metz, B.; Davidson, O.; De Coninck, H.; Loos, M.; Meyer, L., IPCC special report on carbon dioxide capture and storage. Prepared by Working Group III of the Intergovernmental Panel on Climate Change. *IPCC, Cambridge University Press: Cambridge, United Kingdom and New York, USA* **2005,** *4*.

20. Michael, K.; Golab, A.; Shulakova, V.; Ennis-King, J.; Allinson, G.; Sharma, S.; Aiken, T., Geological storage of CO2 in saline aquifers—A review of the experience from existing storage operations. *International Journal of Greenhouse Gas Control* **2010,** *4* (4), 659-667.

21. Markou, G.; Georgakakis, D., Cultivation of filamentous cyanobacteria (blue-green algae) in agro-industrial wastes and wastewaters: A review. *Applied Energy* **2011,** *88* (10), 3389-3401.

22. Znad, H.; Naderi, G.; Ang, H.; Tade, M., *CO2 biomitigation and biofuel production using microalgae: Photobioreactors developments and future directions*. INTECH Open Access Publisher: 2012.

23. Ugwu, C.; Aoyagi, H.; Uchiyama, H., Photobioreactors for mass cultivation of algae. *Bioresource technology* **2008,** *99* (10), 4021-4028.

24. Sarbatly, R. H.; Suali, E., Membrane Photobioreactor as a Device to Increase CO2 Mitigation by Microalgae. In *Advances in Biofuels*, Pogaku, R.; Sarbatly, H. R., Eds. Springer US: Boston, MA, 2013; pp 241-258.

25. Cai, T.; Park, S. Y.; Li, Y., Nutrient recovery from wastewater streams by microalgae: Status and prospects. *Renewable and Sustainable Energy Reviews* **2013,** *19*, 360-369.

26. Brennan, L.; Owende, P., Biofuels from Microalgae: Towards Meeting Advanced Fuel Standards. In *Advanced Biofuels and Bioproducts*, Lee, W. J., Ed. Springer New York: New York, NY, 2013; pp 553-599.

27. Alaswad, A.; Dassisti, M.; Prescott, T.; Olabi, A. G., Technologies and developments of third generation biofuel production. *Renewable and Sustainable Energy Reviews* **2015,** *51*, 1446-1460.

28. Salih, F. M., Microalgae tolerance to high concentrations of carbon dioxide: a review. *Journal of Environmental Protection* **2011,** *2* (05), 648.

29. Gong, J.; You, F., Optimal Design and Synthesis of Algal Biorefinery Processes for Biological Carbon Sequestration and Utilization with Zero Direct Greenhouse Gas Emissions: MINLP Model and Global Optimization Algorithm. *Industrial & Engineering Chemistry Research* **2014,** *53* (4), 1563-1579.

30. Volatile Organic Compounds (VOCs). In *United States Environmental Protection Agency*, 2014.

31. Berenjian, A., N. Chan and H.J. Malmiri, Volatile organic compounds removal methods: A review. *J. Biochem. Biotechnol.* **2012,** *8*, 220-229.

32. Sindelarova, K.; Granier, C.; Bouarar, I.; Guenther, A.; Tilmes, S.; Stavrakou, T.; Müller, J.-F.; Kuhn, U.; Stefani, P.; Knorr, W., Global data set of biogenic VOC emissions

calculated by the MEGAN model over the last 30 years. *Atmospheric Chemistry and Physics* **2014,** *14* (17), 9317-9341.

33. Evuti, A. M., A synopsis on biogenic and anthropogenic volatile organic compounds emissions: hazards and control. *Int. J. Eng* **2013,** *2* (5), 145.

34. Anderson, D., Government Notices - Environment Canada. 2004.

35. Ojala, S.; Pitkäaho, S.; Laitinen, T.; Niskala Koivikko, N.; Brahmi, R.; Gaálová, J.; Matejova, L.; Kucherov, A.; Päivärinta, S.; Hirschmann, C.; Nevanperä, T.; Riihimäki, M.; Pirilä, M.; Keiski, R. L., Catalysis in VOC Abatement. *Topics in Catalysis* **2011,** *54* (16), 1224-1256.

36. Goldstein, A. H.; Galbally, I. E., Known and unexplored organic constituents in the earth's atmosphere. *Environmental Science & Technology* **2007,** *41* (5), 1514-1521.

37. Agency, E. E., Sector share of non-methane volatile organic compounds emissions. 2013.

38. Canada, E., Air Pollutant Emission Inventory (APEI) Report. Environment Canada: 2015.

39. Koppmann, R., Chemistry of Volatile Organic Compounds in the Atmosphere. In *Handbook of Hydrocarbon and Lipid Microbiology*, Timmis, K. N., Ed. Springer Berlin Heidelberg: Berlin, Heidelberg, 2010; pp 267-277.

40. . Volatile Organic Compound Emissions *Environment Canada* [Online], 2014. http://ec.gc.ca/indicateurs-indicators/default.asp?lang=en&n=64B9E95D-1.

41. Khan, F. I.; Kr. Ghoshal, A., Removal of Volatile Organic Compounds from polluted air. *Journal of Loss Prevention in the Process Industries* **2000,** *13* (6), 527-545.

42. Yan, W.; Lien, H.-L.; Koel, B. E.; Zhang, W.-x., Iron nanoparticles for environmental clean-up: recent developments and future outlook. *Environmental Science: Processes & Impacts* **2013,** *15* (1), 63-77.

43. Gomes, H. I.; Dias-Ferreira, C.; Ottosen, L. M.; Ribeiro, A. B., Electrodialytic remediation of polychlorinated biphenyls contaminated soil with iron nanoparticles and two different surfactants. *Journal of colloid and interface science* **2014,** *433*, 189-195.

44. Machado, S.; Stawiński, W.; Slonina, P.; Pinto, A.; Grosso, J.; Nouws, H.; Albergaria, J. T.; Delerue-Matos, C., Application of green zero-valent iron nanoparticles to the remediation of soils contaminated with ibuprofen. *Science of the Total Environment* **2013,** *461*, 323-329.

45. Matlochová, A.; Plachá, D.; Rapantová, N., The application of nanoscale materials in groundwater remediation. *Pol. J. Environ. Stud* **2013,** *22* (5), 1401-1410.

46. Guo, Z.; Ma, R.; Li, G., Degradation of phenol by nanomaterial TiO2 in wastewater. *Chemical Engineering Journal* **2006,** *119* (1), 55-59.

47. . Zero-valent Iron Nanoparticles *US Environmental Protection Agency* [Online], 2014. http://www.epa.gov/rpdweb00/docs/cleanup/nanotechnology/chapter-2-zero-valent.pdf.

48. Crane, R. A.; Scott, T. B., Nanoscale zero-valent iron: Future prospects for an emerging water treatment technology. *Journal of Hazardous Materials* **2012**, 112-125.

49. Li, X.-q.; Elliott, D. W.; Zhang, W.-x., Zero-valent iron nanoparticles for abatement of environmental pollutants: materials and engineering aspects. *Critical reviews in solid state and materials sciences* **2006,** *31* (4), 111-122.

50. Glazier, R.; Venkatakrishnan, R.; Gheorghiu, F.; Walata, L.; Nash, R.; Zhang, W.-x., Nanotechnology takes root. *Civil Engineering* **2003,** *73* (5), 64-69.

51. Henn, K. W.; Waddill, D. W., Utilization of nanoscale zero-valent iron for source remediation—A case study. *Remediation Journal* **2006,** *16* (2), 57-77.

52. Parmar, G. R.; Rao, N. N., Emerging Control Technologies for Volatile Organic Compounds. *Critical Reviews in Environmental Science and Technology* **2008,** *39* (1), 41-78.

53. Eltouny, N.; Ariya, P. A., Competing reactions of selected atmospheric gases on Fe3O4 nanoparticles surfaces. *Physical Chemistry Chemical Physics* **2014**.

54. Mayo, J. T.; Yavuz, C.; Yean, S.; Cong, L.; Shipley, H.; Yu, W.; Falkner, J.; Kan, A.; Tomson, M.; Colvin, V. L., The effect of nanocrystalline magnetite size on arsenic removal. *Science and Technology of Advanced Materials* **2007,** *8* (1–2), 71-75.

55. Chandra, V.; Park, J.; Chun, Y.; Lee, J. W.; Hwang, I.-C.; Kim, K. S., Water-Dispersible Magnetite-Reduced Graphene Oxide Composites for Arsenic Removal. *ACS Nano* **2010,** *4* (7), 3979-3986.

56. Usman, M.; Faure, P.; Ruby, C.; Hanna, K., Remediation of PAH-contaminated soils by magnetite catalyzed Fenton-like oxidation. *Applied Catalysis B: Environmental* **2012,** *117–118* (0), 10-17.

57. Hu, Z.; Beuret, M.; Khan, H.; Ariya, P. A., Development of a recyclable remediation system for gaseous BTEX: Combination of iron oxides nanoparticles adsorbents and electrochemistry. *ACS Sustainable Chemistry & Engineering* **2014,** *2* (12), 2739-2747.

58. Patel, M. R., *Wind and solar power systems: design, analysis, and operation*. CRC press: 2005.

59. Jacobson, M. Z.; Delucchi, M. A., Providing all global energy with wind, water, and solar power, Part I: Technologies, energy resources, quantities and areas of infrastructure, and materials. *Energy Policy* **2011,** *39* (3), 1154-1169.

60. Lewis, N. S., Toward cost-effective solar energy use. *science* **2007,** *315* (5813), 798-801.

61. Köberle, A. C.; Gernaat, D. E. H. J.; van Vuuren, D. P., Assessing current and future techno-economic potential of concentrated solar power and photovoltaic electricity generation. *Energy* **2015,** *89*, 739-756.

62. Jacobson, M. Z., Review of solutions to global warming, air pollution, and energy security. *Energy & Environmental Science* **2009,** *2* (2), 148-173.

63. Wilde, C. Algae carbon uptake and oxygen production potential at high CO_2 concentrations McGill University, Montreal, 2011.

64. Feron, P., H.M.; Hendriks, C., A., *CO_2 Capture Process Principles and Costs*. 2005; Vol. 60, p 451-459.

65. Romera, E.; González, F.; Ballester, A.; Blázquez, M. L.; Muñoz, J. A., Biosorption with Algae: A Statistical Review. *Critical Reviews in Biotechnology* **2006,** *26* (4), 223-235.

66. Vilar, V. J. P.; Botelho, C. M. S.; Boaventura, R. A. R., Methylene blue adsorption by algal biomass based materials: Biosorbents characterization and process behaviour. *Journal of Hazardous Materials* **2007,** *147* (1–2), 120-132.

67. Aravindhan, R.; Rao, J. R.; Nair, B. U., Application of a chemically modified green macro alga as a biosorbent for phenol removal. *Journal of Environmental Management* **2009,** *90* (5), 1877-1883.

68. Wu, Y.-L.; Rahmaningrum, D. G.; Lai, Y.-C.; Tu, L.-K.; Lee, S.-J.; Wang, L.-C.; Chang-Chien, G.-P., Mercury emissions from a coal-fired power plant and their impact on the nearby environment. *Aerosol and Air Quality Research* **2012,** *12* (4), 643-650.

69. LOW-DÉCARIE, E.; Fussmann, G. F.; Bell, G., The effect of elevated CO2 on growth and competition in experimental phytoplankton communities. *Global Change Biology* **2011,** *17* (8), 2525-2535.

70. Bold, H. C., The Morphology of Chlamydomonas chlamydogama, Sp. Nov. *Bulletin of the Torrey Botanical Club* **1949,** *76* (2), 101-108.

71. Bischoff, H. W.; Bold, H. C., *Some soil algae from Enchanted Rock and related algal species*. University of Texas: 1963.

72. Smith, W. F. S. W. F., *Foundations of materials science and engineering*. McGraw-Hill: New York, 1993.

73. Andersen, R. A., *Algal culturing techniques*. Academic press: 2005.

74. Hudson, E.; Okuda, K.; Ariya, P., Determination of acetone in seawater using derivatization solid-phase microextraction. *Anal Bioanal Chem* **2007,** *388* (5-6), 1275-1282.

75. Hudson, E. D.; Ariya, P. A.; Gelinas, Y., A method for the simultaneous quantification of 23 C-1-C-9 trace aldehydes and ketones in seawater. *Environmental Chemistry* **2011,** *8* (4), 441-449.

76. Panel, I. *The Fifth Assessment Report (AR5) of the United Nations Intergovernmental Panel on Climate Change (IPCC), Climate Change 2013: The Physical Science Basis, IPCC WGI AR5*; Tech. rep., Intergovernmental Panel on Climate Change (IPCC): 2013.

77. WMO, The state of greenhouse gases in the atmosphere using global observations through 2011. *Greenhouse Gas Bulletin* **2012,** (8), 1-4.

78. Core Writing Team, P., R.K. and Reisinger, A. (Eds.) *Contribution of Working Groups I, II and III to the Fourth Assessment Report of the Intergovernmental Panel on Climate Change*; IPCC: Switzerland, 2007; p 104.

79. Agency, I. E., CO2 Emissions from Fuel Combustion. *IEA Statistics* **2011**.

80. van der Zwaan, B.; Smekens, K., CO2 capture and storage with leakage in an energy-climate model. *Environmental modeling & assessment* **2009,** *14* (2), 135-148.

81. Forster, P.; Ramaswamy, V.; Artaxo, P.; Berntsen, T.; Betts, R.; Fahey, D. W.; Haywood, J.; Lean, J.; Lowe, D. C.; Myhre, G., Changes in atmospheric constituents and in radiative forcing. Chapter 2. In *Climate Change 2007. The Physical Science Basis*, 2007.

82. Houghton, J. T.; Ding, Y.; Griggs, D. J.; Noguer, M.; van der Linden, P. J.; Dai, X.; Maskell, K.; Johnson, C., *Climate change 2001: the scientific basis*. Cambridge university press Cambridge: 2001; Vol. 881.

83. Pires, J. C. M.; Alvim-Ferraz, M. C. M.; Martins, F. G.; Simões, M., Carbon dioxide capture from flue gases using microalgae: Engineering aspects and biorefinery concept. *Renewable and Sustainable Energy Reviews* **2012,** *16* (5), 3043-3053.

84. Packer, M., Algal capture of carbon dioxide; biomass generation as a tool for greenhouse gas mitigation with reference to New Zealand energy strategy and policy. *Energy Policy* **2009,** *37* (9), 3428-3437.

85. Gale, J.; Freund, P. In *Greenhouse gas abatement in energy intensive industries*.

86. Wang, S.; Sun, H.; Ang, H. M.; Tadé, M. O., Adsorptive remediation of environmental pollutants using novel graphene-based nanomaterials. *Chemical Engineering Journal* **2013,** *226* (0), 336-347.

87. Joseph, Y.; Wühn, M.; Niklewski, A.; Ranke, W.; Weiss, W.; Wöll, C.; Schlögl, R., Interaction of ethylbenzene and styrene with iron oxide model catalyst films at low coverages: A NEXAFS study. *Physical Chemistry Chemical Physics* **2000,** *2* (22), 5314-5319.

88. Ye, C. Z.; Ariya, P. A., Co-adsorption of gaseous benzene, toluene, ethylbenzene, m-xylene (BTEX) and SO2 on recyclable Fe3O4 nanoparticles at 0–101% relative humidities. *Journal of Environmental Sciences* **2015,** *31* (0), 164-174.

89. Eltouny, N.; Ariya, P. A., Enhanced Reactivity toward Oxidation by Water Vapor: Interactions of Toluene and NO2 on Hydrated Magnetite Nanoparticles. *The Journal of Physical Chemistry C* **2014,** *118* (41), 23654-23663.

90. Eltouny, N.; Ariya, P. A., The Impact of Chemical Aging on Ice Nucleating Abilities of Iron Oxide Nanoparticles in the Atmosphere. In *Nucleation and Atmospheric Aerosols*, DeMott, P. J.; Odowd, C. D., Eds. 2013; Vol. 1527, pp 930-932.

91. Eltouny, N. A.; Ariya, P. A., Fe3O4 Nanoparticles and Carboxymethyl Cellulose: A Green Option for the Removal of Atmospheric Benzene, Toluene, Ethylbenzene, and o-Xylene (BTEX). *Industrial & Engineering Chemistry Research* **2012,** *51* (39), 12787-12795.

92. Snider, G.; Ariya, P., Photo-catalytic oxidation reaction of gaseous mercury over titanium dioxide nanoparticle surfaces. *Chemical Physics Letters* **2010,** *491* (1-3), 23-28.

93. Snider, G.; Ariya, P., Kinetic and Product Studies of the Reactions of NO2, with Hg-0 in the Gas Phase in the Presence of Titania Micro-Particle Surfaces. *Water Air and Soil Pollution* **2012,** *223* (7), 4397-4406.

94. Snider, G.; Raofie, F.; Ariya, P. A., Effects of relative humidity and CO(g) on the O(3)-initiated oxidation reaction of Hg(0)(g): kinetic & product studies. *Physical Chemistry Chemical Physics* **2008,** *10* (36), 5616-5623.

95. Biofuels, N. R. C. C. o. t. S. D. o. A., *Sustainable Development of Algal Biofuels in the United States*. National Academies Press: 2012.

96. Massart, R., Preparation of aqueous magnetic liquids in alkaline and acidic media. *IEEE transactions on magnetics* **1981**, 1247-1248.

97. Subir, M.; Eltouny, N.; Ariya, P. A., A surface second harmonic generation investigation of volatile organic compound adsorption on a liquid mercury surface. *RSC Advances* **2015,** *5* (30), 23464-23470.

98. Deeds, D. A.; Ghoshdastidar, A.; Raofie, F.; Guérette, É.-A.; Tessier, A.; Ariya, P. A., Development of a Particle-Trap Preconcentration-Soft Ionization Mass Spectrometric Technique for the Quantification of Mercury Halides in Air. *Analytical chemistry* **2015**.

99. Swanson, H.; McMurdie, H.; Morris, M.; Evans, E.; Paretzkin, B., National Bureau of Standards Monograph 25. *Section* **1972,** *10*, 161.

100. Thomas, D. J.; Sullivan, S. L.; Price, A. L.; Zimmerman, S. M., Common freshwater cyanobacteria grow in 100% CO2. *Astrobiology* **2005,** *5* (1), 66-74.

101. Jacob-Lopes, E.; Gimenes Scoparo, C. H.; Queiroz, M. I.; Franco, T. T., Biotransformations of carbon dioxide in photobioreactors. *Energy Conversion and Management* **2010,** *51* (5), 894-900.

102. Gribble, G. W., Naturally Occurring Organohalogen Compounds--A Survey. *Journal of Natural Products* **1992,** *55* (10), 1353-1395.

103. Keppler, F.; Eiden, R.; Niedan, V.; Pracht, J.; Scholer, H. F., Halocarbons produced by natural oxidation processes during degradation of organic matter. *Nature* **2000,** *403* (6767), 298-301.

104. Von Salzen, K.; Leighton, H.; Ariya, P.; Barrie, L.; Gong, S.; Blanchet, J.-P.; Spacek, L.; Lohmann, U.; Kleinman, L., Sensitivity of sulphate aerosol size distributions and CCN concentrations over North America to SOx emissions and H2O2 concentrations. *Journal of geophysical research* **2000,** *105* (D8), 9741-9765.

105. EPA Dimethyl Phthalate. http://www.epa.gov/ttnatw01/hlthef/dimet-ph.html#ref2.

106. EPA Styrene. http://www.epa.gov/ttnatw01/hlthef/styrene.html.

107. de la Noüe, J.; Laliberté, G.; Proulx, D., Algae and waste water. *Journal of Applied Phycology* **1992,** *4* (3), 247-254.

108. Vilar, V. J. P.; Botelho, C. M. S.; Boaventura, R. A. R., Equilibrium and kinetic modelling of Cd(II) biosorption by algae Gelidium and agar extraction algal waste. *Water Research* **2006,** *40* (2), 291-302.

109. Bulgariu, D.; Bulgariu, L., Equilibrium and kinetics studies of heavy metal ions biosorption on green algae waste biomass. *Bioresource Technology* **2012,** *103* (1), 489-493.

110. Lata, S.; Singh, P. K.; Samadder, S. R., Regeneration of adsorbents and recovery of heavy metals: a review. *International Journal of Environmental Science and Technology* **2015,** *12* (4), 1461-1478.

111. Hu, Z.; Kurien, U.; Murwira, K.; Ghoshdastidar, A.; Nepotchatykh, O.; Ariya, P. A., Development of a Green Technology for Mercury Recycling from Spent Compact Fluorescent Lamps Using Iron Oxides Nanoparticles and Electrochemistry. *ACS Sustainable Chemistry & Engineering* **2016,** *4* (4), 2150-2157.

112. Valdés, F. J.; Hernández, M. R.; Catalá, L.; Marcilla, A., Estimation of CO2 stripping/CO2 microalgae consumption ratios in a bubble column photobioreactor using the analysis of the pH profiles. Application to Nannochloropsis oculata microalgae culture. *Bioresource Technology* **2012,** *119*, 1-6.

113. Sirikulrat, K.; Koonaphapdeelert, S., Capture of Carbon Dioxide in Biogas by using Chlorella sp. in Photobioreactor.

114. Sobczuk, T. M.; Camacho, F. G.; Rubio, F. C.; Fernández, F.; Grima, E. M., Carbon dioxide uptake efficiency by outdoor microalgal cultures in tubular airlift photobioreactors. *Biotechnology and bioengineering* **2000,** *67* (4), 465-475.

115. Feron, P., H.M.; Hendriks, C., A., Les différents procédés de capture du CO2 et leurs coûts. *Oil & Gas Science and Technology - Rev. IFP* **2005,** *60* (3), 451-459.

116. Chen, C.-Y.; Yeh, K.-L.; Aisyah, R.; Lee, D.-J.; Chang, J.-S., Cultivation, photobioreactor design and harvesting of microalgae for biodiesel production: a critical review. *Bioresource technology* **2011,** *102* (1), 71-81.

117. Association, C. E., Key Canadian Electricity Statistics 2014. 2014.

118. Toronto, C. o. Water Rates. http://www1.toronto.ca/wps/portal/contentonly?vgnextoid=a916ff0e43db1410VgnVCM10000071d60f89RCRD&vgnextchannel=1c4bfd788a5af310VgnVCM10000071d60f89RCRD.

119. Eco Global Fuels USA, L. Comparative Analysis: Conventional Hydrogen Production. http://ecoglobalfuels.com/Technology/comparative-analysis (accessed October 2014).

120. Ellis, J. T.; Hengge, N. N.; Sims, R. C.; Miller, C. D., Acetone, butanol, and ethanol production from wastewater algae. *Bioresource Technology* **2012,** *111* (0), 491-495.

121. Rubin, E. S.; Mantripragada, H.; Marks, A.; Versteeg, P.; Kitchin, J., The outlook for improved carbon capture technology. *Progress in Energy and Combustion Science* **2012,** *38* (5), 630-671.

122. McCoy, S. T.; Rubin, E. S., Variability and uncertainty in the cost of saline formation storage. *Energy Procedia* **2009,** *1* (1), 4151-4158.

8. Appendix

List of Figures

8.1. Characterization of algae and cyanobacteria species

Algal samples were imaged by high resolution scanning electron microscopy (HR-SEM), to visualize their surface topology, morphological structures and relative sizes. As portrayed in Figure A.1, all species were found to be unicellular microalgae, with the cyanobacteria strains being smaller in size than the green algae. Both cyanobacteria species revealed to have similar dimensions, of approximately 6-7 µm in length, and were prolate spheroidal. *Scenedesmus sp.* displayed spherical cells of about 10 µm in diameter with a generally smooth surface. *Chlamydomonas reinhardtii* displayed more extracellular products surrounding the cells compared to the other samples. Optical pictures, in Figure A.2(a), show the presence of flagella which could be a reason for the additional material surrounding this algal species. Their wrinkly texture could also indicate that the sample was at a later stage in growth. *Chlamydomonas reinhardtii* cells appeared to have spheroidal structures, of around 6 µm in length.

From the species obtained, *Anabaena sp.* and *Scenedesmus sp.* demonstrated to be the most tolerant to significantly high concentrations of CO_2; however the latter species could not sustain growth for longer than two days at 60 % CO_2. Due to the *Anabaena sp.* cells' smaller size, appearing to show greater surface to volume aspect ratio than *Scenedesmus sp.*, and its greater tolerance to high CO_2 concentrations; it was chosen for further experimentation for the analysis of the by-products at the outlet gas stream of the photo-bioreactor.

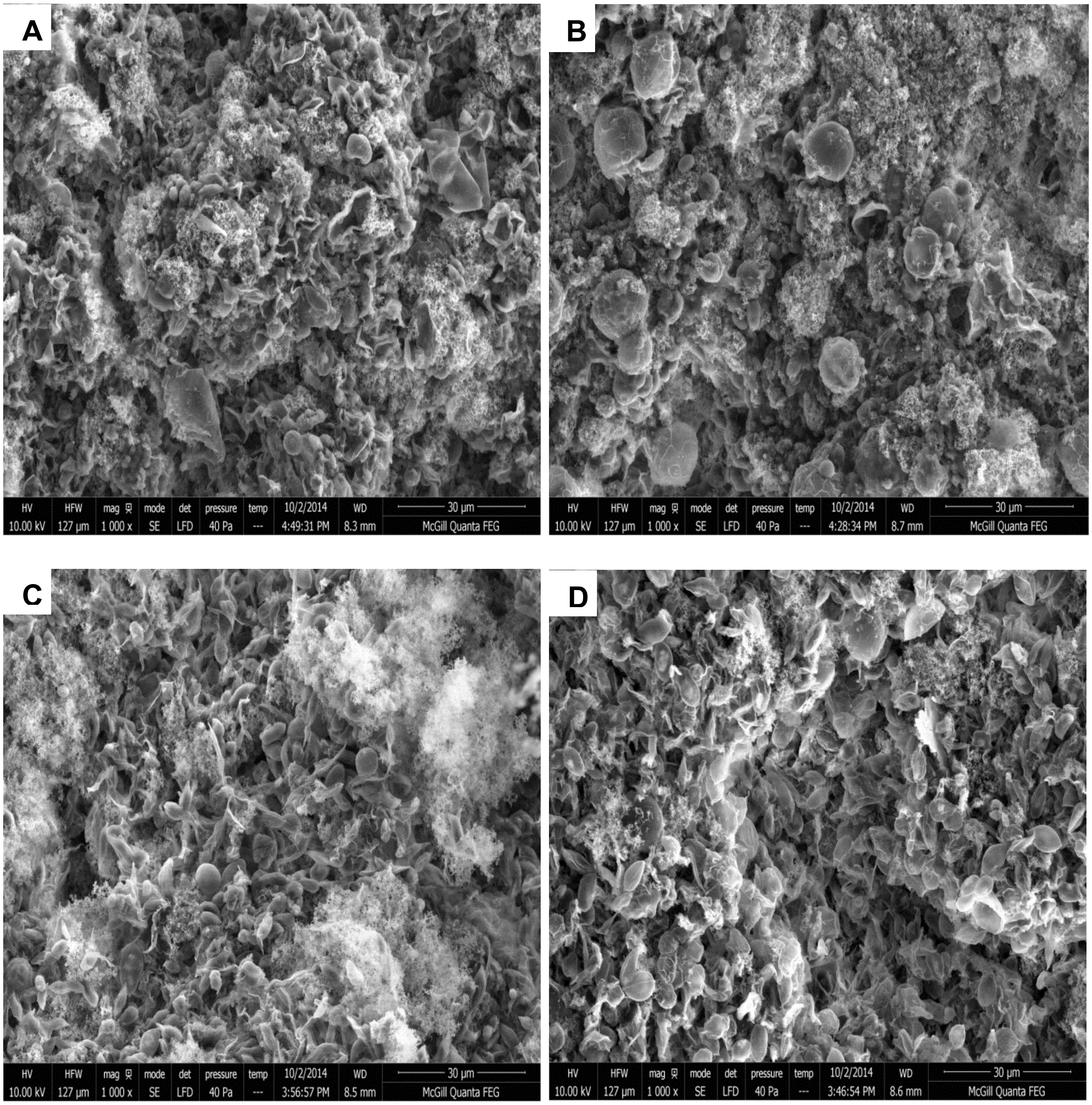

Figure A.1. High resolution scanning electron microscopy (HR-SEM) images of: green algae a) *Chlamydomonas reinhardtii*; b) *Scenedesmus sp.*; and cyanobacteria c) *Anabaena sp.*; d) *Synechococcus sp.* (Mag.: 1000x)

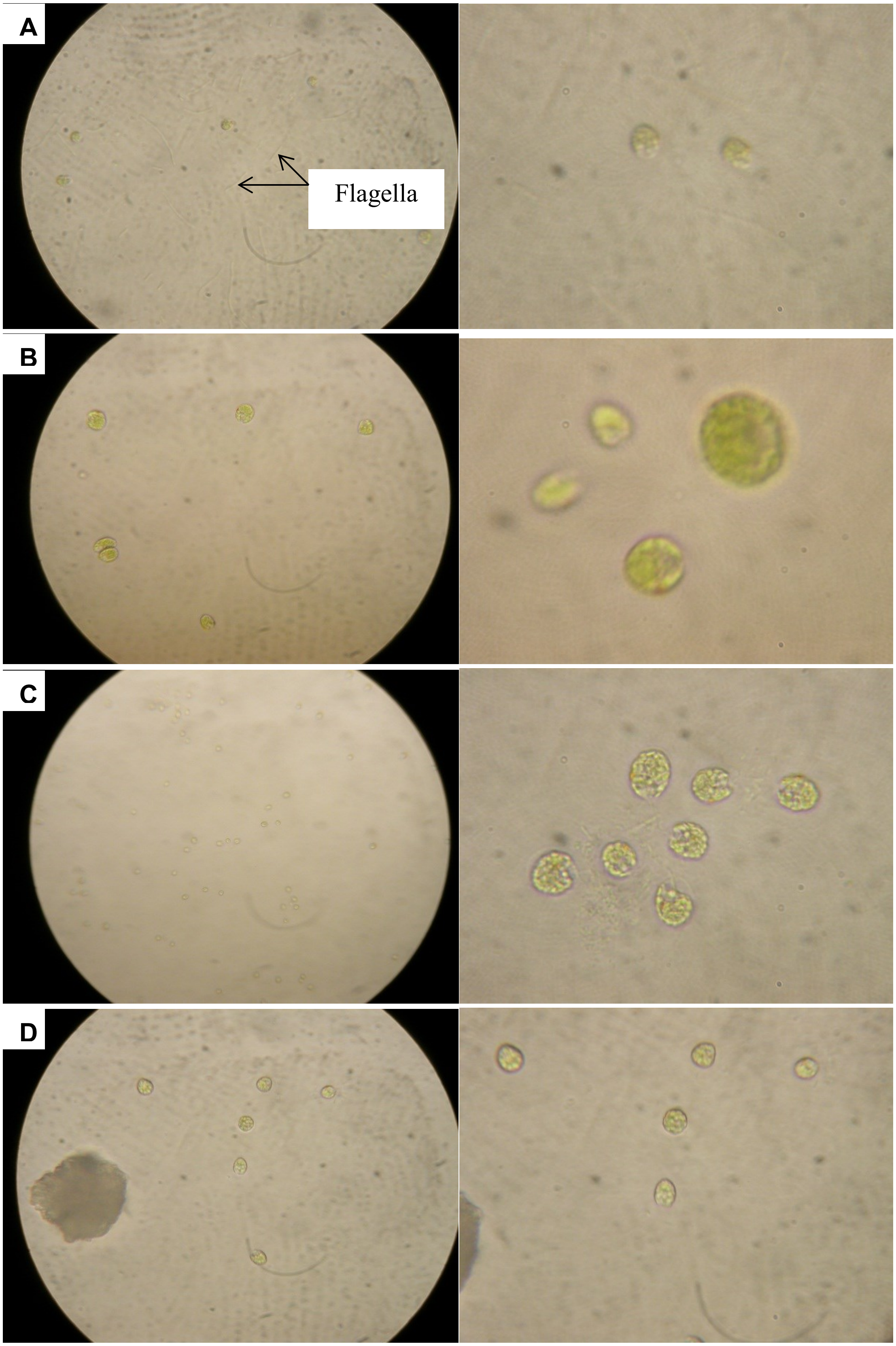

Figure A.2. Optical microscopy images of: a) *Chlamydomonas reinhardtii*; b) *Scenedesmus sp.*; c) *Anabaena sp.*; d) *Synechococcus sp.*

Note: (Microscope mag. 100x, and additional image zoom with camera zoom)

8.2. Relative Humidity Tests

Relative humidity measurements, as depicted in Figure A.3, show that relative humidity in the outlet gas stream of the PBR was substantial, of about 90 % at a temperature of 23.3 ± 1.5 °C. The aluminum oxide trap proved to be effective in reducing the water vapour from the gas stream to about 4 %. It is essential for the trap to be upstream of the iron oxide interfaces, since high water vapour content has been shown to deactivate the surface of iron oxide particles due to preferential adsorption of water molecules onto the active sites of the adsorbent.[88-89] Competitive adsorption between water molecules and VOCs present in this work has not been previously documented. To understand the extent on influence of water vapour on the adsorption of VOCs, reported herein, additional studies are required to further optimize the system. Subsequent removal of water molecules from the iron oxide surfaces could be performed by heat treatment or vacuum drying. After a period of 8 hours approximately, effluent gas stream after the aluminum oxide traps would contain about 70 % relative humidity. Hence each time the iron oxide interface experiments were performed, this trap was packed with new aluminum oxide pellets.

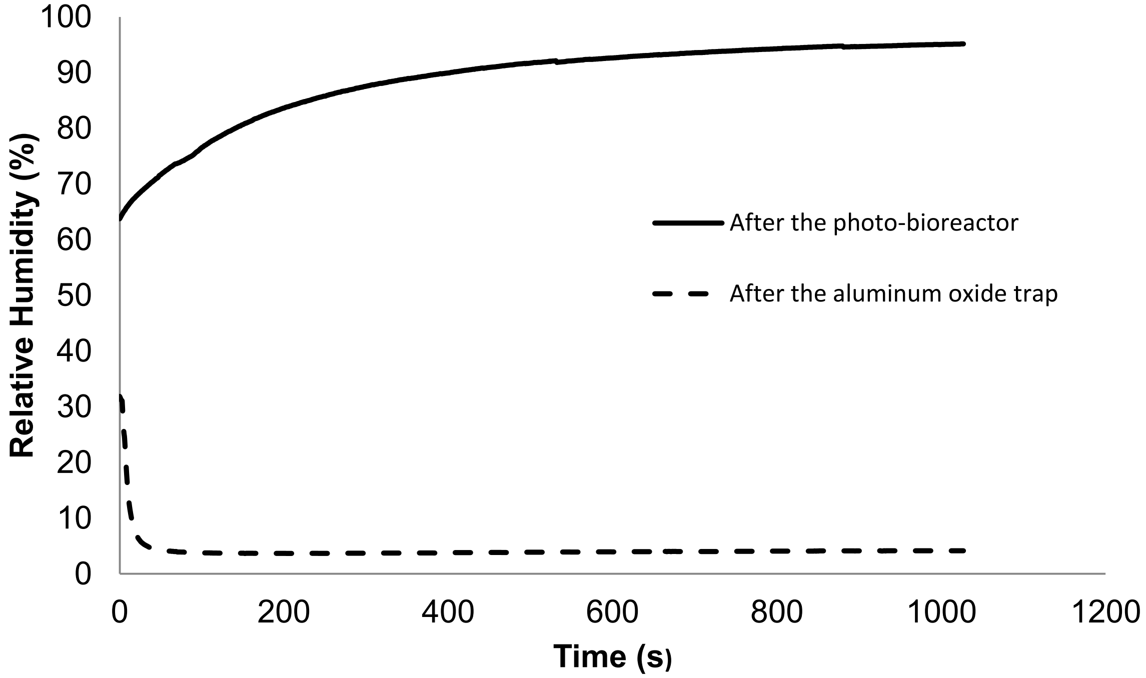

Figure A.3. Humidity of the gas stream before and after aluminum oxide trap

8.3. Additional Figures

8.3.1. Typical derivatization chromatogram from algal headspace

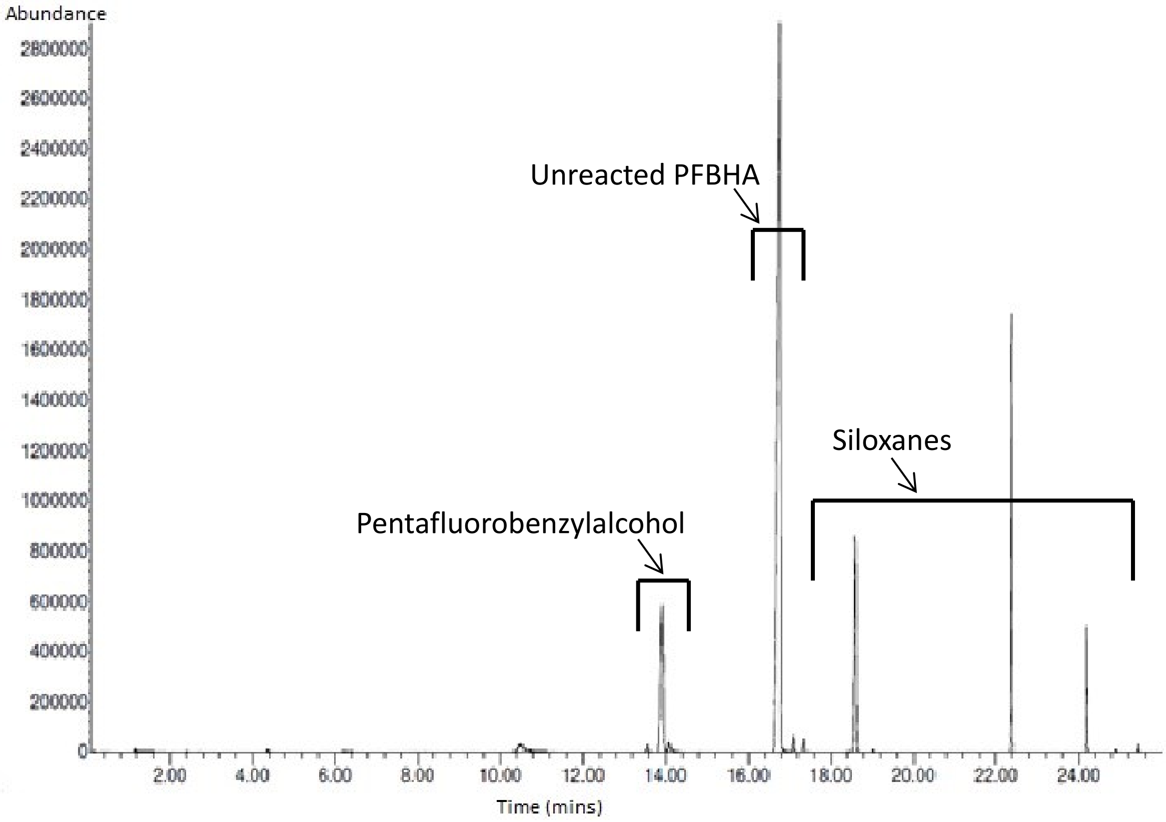

Figure A.4. An example of derivatization with headspace-SPME-GC-MS (black fibre)

8.3.2. <u>FE-SEM of commercial magnetite microparticles</u>

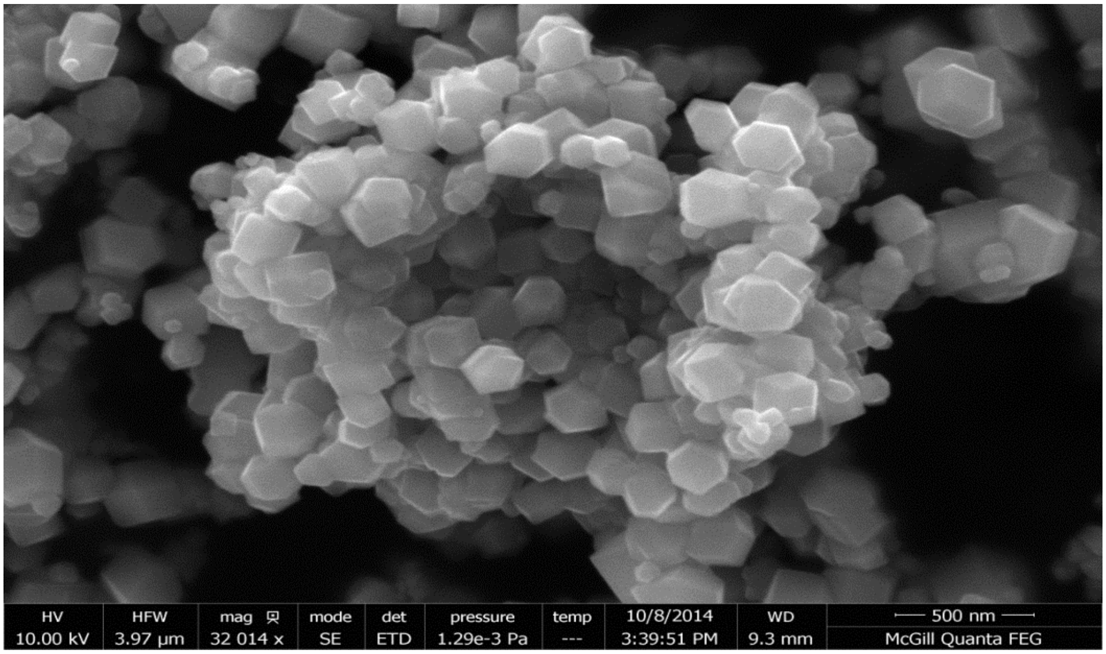

Figure A.5. Field emission scanning electron microscopy (FE-SEM) image of commercial magnetite particles, also tested as an adsorbent

8.3.3. Optical microscopy images of algae coupled with their UV-spectra

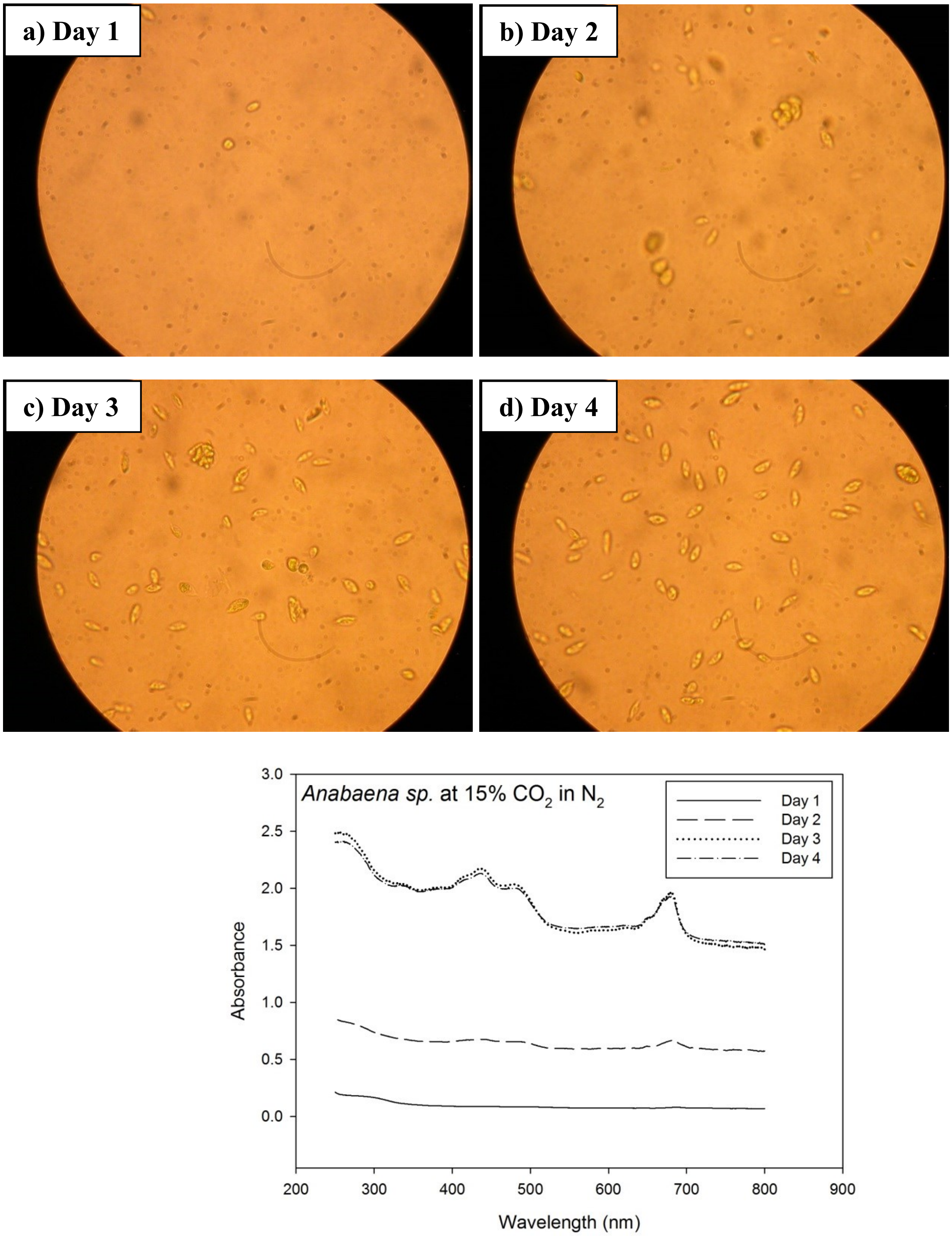

Figure A.6. Optical microscopy images of *Anabaena sp.* at 15% CO_2 in N_2 at different growth stages, coupled with the UV spectra.

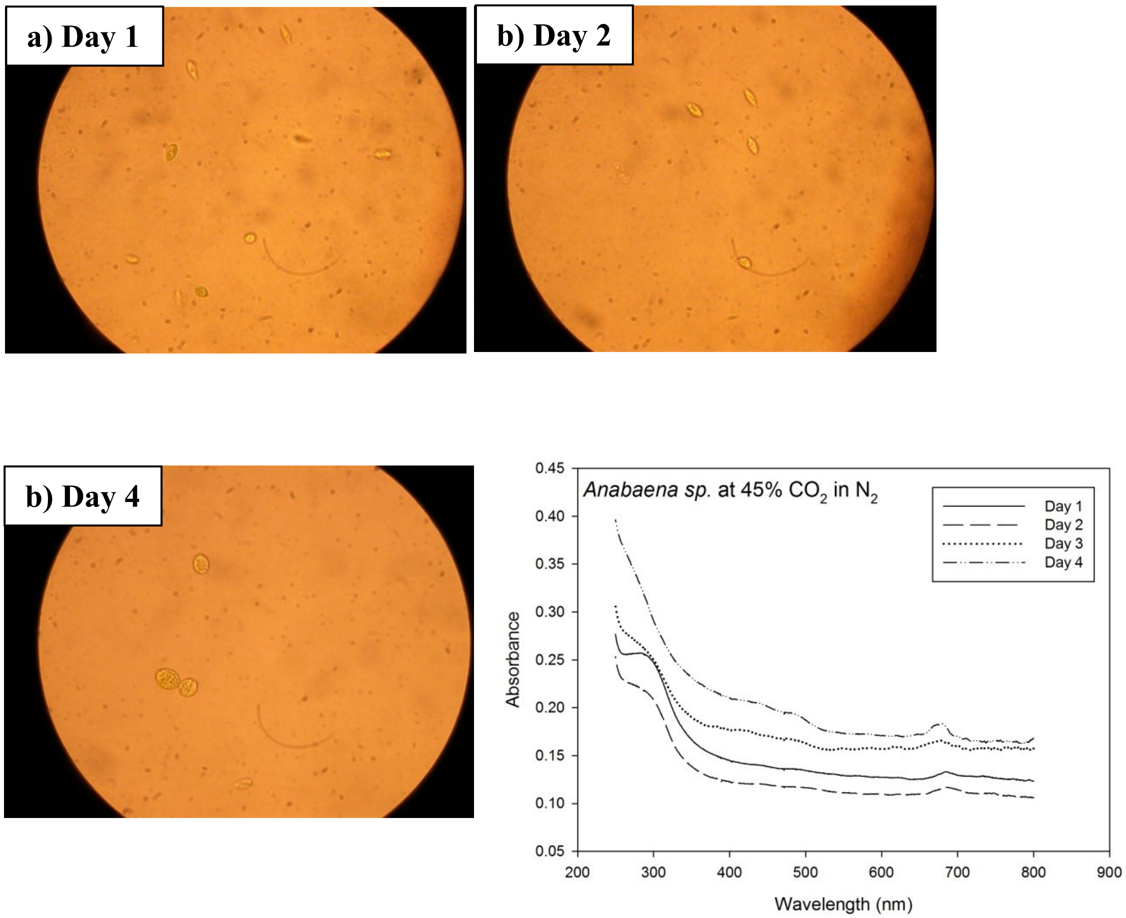

Figure A.7. Optical microscopy images of *Anabaena sp.* at 45% CO_2 in N_2 at different growth stages, coupled with their UV spectra.

Note: Algae at 45% CO_2 grew predominantly along the top and bottom sections of the PBR walls, and settled at the bottom of the PBR (with the bulk liquid maintaining a clear colour). Thus the amount of suspended algae in the liquid was not seen to increase over time.

8.4. Solar panel power availability

A current-voltage curve was specified for the PV module to determine the available power from different combinations of current (I) and voltage (V). The power is determined from the product of voltage and current at any point along the curve. The maximum power obtained from the graph is approximately 170 W at 26 V, greater than the power required for the set-up (120 W). Figure A.8 below shows the I-V curve obtained from the PV panel.

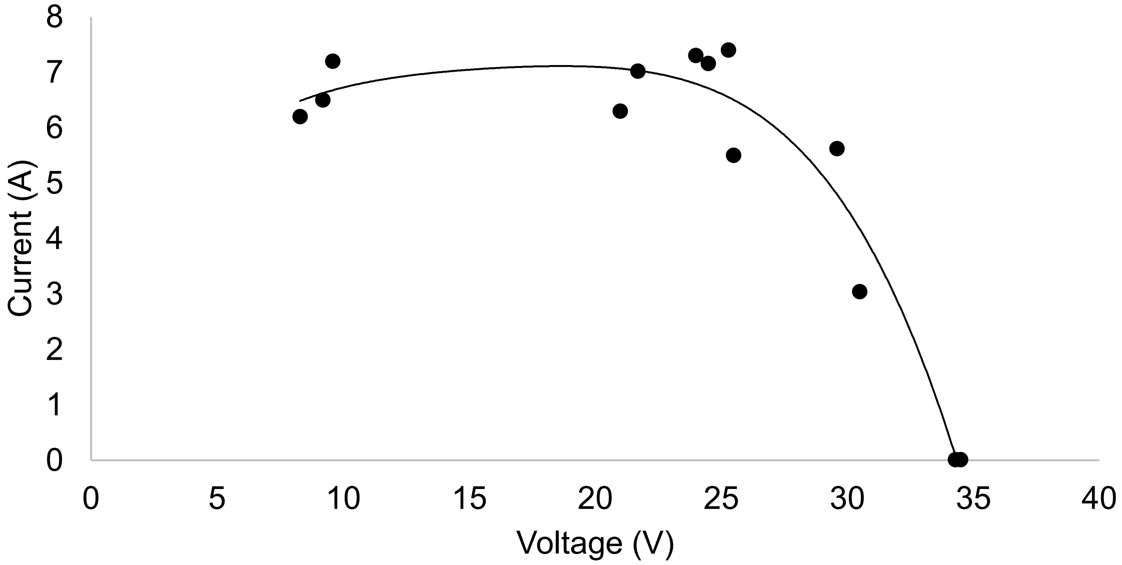

Figure A.8. Current - Voltage curve of Solar (PV) Panel